HYBRID ENERGY STORAGE TO INCREASE DURABILITY AND EFFICIENCY OF HYBRID ELECTRIC VEHICLES

by

Wehan Louw

Submitted in partial fulfillment of the requirements for the degree
Master of Engineering (Electrical Engineering)

in the

Department of Electrical, Electronic and Computer Engineering
Faculty of Engineering, Built Environment and Information Technology

UNIVERSITY OF PRETORIA

February 2022

SUMMARY

HYBRID ENERGY STORAGE TO INCREASE DURABILITY AND EFFICIENCY OF HYBRID ELECTRIC VEHICLES

by

Wehan Louw

Supervisor:	Prof. W. P. du Plessis
Department:	Electrical, Electronic and Computer Engineering
University:	University of Pretoria
Degree:	Master of Engineering (Electrical Engineering)
Keywords:	Hybrid electric vehicles, supercapacitors, emissions, fuel economy, energy management, energy storage, battery management systems.

Electric vehicles are one of the industries being pushed to phase out combustion engines for countries to achieve their goal of reducing emissions. Some countries however cannot complete this transition as smooth and swiftly, and South Africa is one example. South Africa's electricity grid is struggling to keep up with the demand, and thus has to implement load shedding and scheduling. For this reason, hybrid electric vehicles (HEVs) will be investigated. HEVs use lithium-ion (Li-ion) batteries which have a limited number of charge cycles. These batteries are also much smaller in HEVs than in electric vehicles (EVs), thus undergoing full charge cycles more frequently.

It was proposed to add an additional short-term energy storage system to be implemented in unison with the battery to reduce fuel consumption, reduce emission, and increase the service life of the battery. A quasi-static simulation approach was used to create and simulate the models using the QSS Toolbox developed by ETH Zürich. To compare results a model was defined with similar specifications to a Toyota Yaris Hybrid and achieved similar fuel consumption results. This is referred to as the reference model without the supercapacitor added.

The proposed vehicle with a supercapacitor of about 5% of the battery size was modelled. The implementation of the supercapacitor and the design of a power distribution controller was guided by knowledge gained throughout the study. The supercapacitor was utilised as a power peak shaving solution to reduce the load on the battery in high-demand instances. The proposed HEV model produced results with both fuel consumption and emissions reduced by up to 23%, especially in urban conditions. It also showed promise in increasing the life of the battery by reducing the charge cycles required to complete an urban drive cycle.

ACKNOWLEDGEMENTS

I would like to thank my parents for their everlasting patience, love and support throughout all my years of study.

I am very grateful for my supervisor, Prof. Warren du Plessis, who has continued to provide me with motivational support and feedback through this process to ensure I give my absolute best.

Many thanks to all my friends and family that remained patient when I could not join them for all the activities they planned when I had to study.

Special thanks to Me. Gous, who has always been extremely supportive and quick to handle my admin-related enquiries.

Finally, I thank the Lord for blessing me with the privilege to be able to have done something like this, and for surrounding me with all the people who provide endless love and support.

LIST OF ABBREVIATIONS

AC	alternating current
CO	carbon monoxide
CO_2	carbon dioxide
DC	direct current
EDLC	electric double layer cpacitor
EPA	Environmental Protection Agency
EV	electric vehicle
FESS	flywheel energy storage system
FTP	Federal Test Procedure
GPS	Global Positioning System
GUI	graphical user interface
HC	hydrocarbon
HESS	hybrid energy storage system
HEV	hybrid electric vehicle
HPF	high-pass filter
HWFET	Highway Fuel Economy Test
ICE	internal combustion engine
Li-ion	lithium-ion
LPF	low-pass filter
NO_x	nitrogen oxide
PM	particulate matter
PV	photovoltaic
QSS	QuasiStatic Simulation Toolbox
SARS	South African Revenue Service
SOC	state of charge
THC	total hydrocarbon content

UK	United Kingdom
ZAR	South African Rand

TABLE OF CONTENTS

LIST OF FIGURES

LIST OF TABLES

CHAPTER 1 INTRODUCTION

1.1 PROBLEM STATEMENT

1.1.1 Context of the problem

Vehicles driven by internal combustion engines (ICEs) are one of the main contributors to air pollution which is harmful to human health and the environment. ICEs emit gasses during the combustion process and are released into the air. These pollutants include carbon monoxide (CO), carbon dioxide (CO_2), nitrogen oxide (NO_x), hydrocarbon (HC) and particulate matter (PM). From an environmental perspective, it could negatively impact climate which in turn could affect agriculture. Crop yield can be hindered by undesirable conditions such as droughts, heatwaves and floods [1]. Effects on human health can vary from sensory irritation to symptoms affecting respiratory or cardiovascular systems, or even cancer, [2].

Hybrid electric vehicles (HEVs) offer a more financially stable environment for transport. HEVs are lighter on fuel and are less susceptible to being influenced by global impact factors such as oil prices. Even more so are full electric propulsion vehicles which are completely fuel independent [3].

South Africa's electricity network is struggling to keep up with the demand, causing interrupted supply. Therefore a significant increase in electric vehicles is inadvisable, as it would amount to additional strain on the electricity utility [4]. It is believed that if an electric vehicle (EV) were to be charged from the local grid it would be generating more emissions than a modern ICE vehicle [5].

This is where HEVs could be a potential solution, it provides significant fuel consumption reductions and is not as, or sometimes not at all dependent on the electricity grid. HEVs have proven that they have much better fuel economy and reduced emission when compared to conventional ICE vehicles [6].

This makes it the ideal candidate for a transition to cleaner energy vehicles in a country such as South Africa without adding strain to the electricity grid.

A concern with EVs and HEVs is that the batteries are a fairly expensive component and as such, they should last as long as possible before requiring a replacement. A contributing factor that reduces battery service life is strain caused by high power demand. This limits the efficacy of a battery's ability to reduce fuel consumption unless the battery is oversized [7]. An in-depth study will be done to determine if an additional energy storage component could be a potential solution to solve these concerns. This additional energy storage component will be a short-term energy storage system. The short-term energy storage system in this dissertation is defined as a component that is capable of storing energy, but holds a small charge capacity. Its primary purpose would be to deploy bursts of power under high demand conditions.

1.1.2 Research gap

It became apparent from studies mentioned in Section 2.4, that series HEV models are not as popular as parallel or combined HEV configurations. This sparks curiosity to further investigate this configuration, since it is the closest variation of HEVs to full EVs. This means that the series HEV configuration should be best suited for the scope of this study.

This study investigates the use of short-term energy storage in HEVs by providing an updated and modernised HEV model featuring a lithium-ion (Li-ion) battery and a non-time-restricted charge controller. Two short-term energy storage systems were compared to motivate the selection of a supercapacitor. Integration of the supercapacitor was then implemented, in which the power required by the battery is reduced in order to increase the battery's life expectancy. This requires the design of a power-management controller and its addition to the HEV model. Additionally, a production HEV's specifications are applied to the model, and simulations are performed using Federal Test Procedure (FTP) drive cycles in both urban and highway environments to ensure that results are both realistic and relevant. The proposed model with the additional supercapacitor will then be compared to this reference model to determine the effect of adding an additional short-term storage system. Finally, the implications of the supercapacitor on fuel consumption and emissions are considered.

1.2 RESEARCH OBJECTIVE AND QUESTIONS

1.2.1 Two-part primary question

- Is it possible to use the QSS toolbox simulation software to simulate a HEV with an additional energy storage system to support the battery under high power demand conditions?

- If so, what modifications and additional components would be required to construct such a model?

This two-part question defines the objective of the study because if the answer to this question is not satisfied the secondary questions could not be answered.

1.2.2 Secondary questions

- Will the proposed system be able to increase the service life of the HEV's battery?

One of the main objectives is to determine if the life of the battery can be extended. If the proposed system reduces the strain on the battery it should result in a healthier battery for longer.

- How does the proposed model with an additional energy storage compare to a model without an additional storage system in terms of fuel economy and reduced emissions?

It is expected that the additional energy storage system, with a high power density, would reduce the strain on the battery during high power demand scenarios. Reducing the rate of discharge of the battery in a series hybrid configuration should require reduced ICE assistance.

- How will different drive cycles affect the behaviour of the proposed vehicle?

An urban drive cycle should be more power-demanding based on the frequency of acceleration and deceleration, which might utilise the extra energy storage more, when compared to a highway driving environment.

- How will the additional storage system and the additional required components to accommodate it affect the total cost of the hybrid electric vehicle and could the benefits justify the additional cost?

The addition of a secondary energy storage system will surely have financial implications. The objective is to determine the additional cost and identify the potential cost savings the proposed vehicle provides.

1.3 APPROACH

A simulation software had to be chosen which had the capability to easily modify components and models. The QuasiStatic Simulation Toolbox (QSS) toolbox was the best-suited software for this study due to the flexibility and compatibility it provides but it has some outdated components, such as a lead acid battery model. The QSS toolbox has been used in previous publications and is also used in masters degree projects [8–12].

The model was updated to use a Li-ion battery. It was decided that instead of using the software's preset vehicle parameters, the model had to resemble the specifications of a real-world HEV. The Toyota Yaris Hybrid was chosen and all the parameters of the simulation model were adjusted to match its specifications. The simulations were performed using city and highway drive cycles to resemble a combined fuel economy result. It was proven that the reference model created could achieve accurate results and almost matched the claimed fuel consumption of a Toyota Yaris Hybrid.

It was decided that the secondary energy storage unit will be a supercapacitor. The supercapacitor had to be implemented in a parallel configuration to the battery to ensure both components can operate independently. This required that a new controller had to be designed to manage the flow of power between the two energy storage systems. The controller used the power peak shaving method which is quite common in energy optimisation [13], [14]. The new vehicle model was then simulated using the same drive cycles. The results obtained were analysed and discussed. The advantages and cost implications were also documented while summarising the outcome of this study.

1.4 RESEARCH GOALS

- Gain knowledge of the different control strategies and how to implement at least one of these methods. Understanding how the control strategies correlate with the configurations in which the hybrid energy storage system (HESS) can be constructed.
- Understanding the impact an additional energy storage unit combined with a Li-ion battery will have on various factors. These include battery longevity, vehicle travelling range and vehicle emissions.
- Determine whether the cost of using a HESS compared to battery-only energy storage in HEVs is viable.

1.5 RESEARCH CONTRIBUTION

- An in-depth investigation of how the QSS toolbox works, ensured the knowledge was obtained to be able to modify and add additional components to a vehicle model. This allowed for outdated models to be modernised with newer technology such as a Li-ion battery and dynamically controlled battery controller. The simulation method is understood, which allowed for new compatible components to be added to create the proposed model.
- It was determined that a HEV modelled in the QSS toolbox was able to achieve comparable results to a real-world Toyota Yaris Hybrid. This ensured that the reference model used to compare the proposed model provided an accurate baseline.
- Knowledge and understanding of the study made it clear that the implementation of a secondary energy storage system had to be done in a parallel configuration to the battery. This allows for individual control with a power management controller.
- From the research it was made clear that a power peak shaving, also known as a high-pass filter/low-pass filter (HPF/LPF) control method ,is a common way to manage power flow between two energy storage systems. The design and implementation of this controller could effectively reduce the peak power required from the battery and supply the remaining power from the supercapacitor.
- The results were discussed, showing improvements in terms of fuel economy and emission. This is especially true for urban environments. It was also discussed how the proposed system increased the potential battery service life.

1.6 RESEARCH OUTCOMES

A journal article was compiled using the research obtained in this study and was submitted to the IEEE Transactions on Transportation Electrification.

Authors: Wehan Louw and Prof. Warren P. du Plessis.

Title: Decreasing Peak Load And Increasing Service Life Of Batteries Of Hybrid Electric Vehicles By Addition Of Temporary Energy Storage.

Abstract: The addition of a short-term energy-storage system in conjunction with the battery to reduce fuel consumption, reduce emissions, and increase the service life of the battery is considered. A quasi-static simulation approach was used to simulate the models using the QuasiStatic Simulation Toolbox (QSS) developed by ETH Zürich. In order to compare results, a model was defined with similar specifications to a Toyota Yaris Hybrid, and similar fuel consumption results were achieved. A supercapacitor of about 5% of the battery size was chosen and implemented together with a power distribution controller. The supercapacitor was utilised as a power peak shaving solution to reduce the load on the battery in high-demand instances. The proposed hybrid electric vehicle (HEV) model produced results with improved fuel consumption and emissions reductions of up to 23%, especially under urban conditions. This system also showed promise in increasing the life of the battery by reducing the charge cycles required to complete an urban drive cycle.

It was however not accepted and published. The feedback was used to improve the detail in which content and results are presented in this dissertation.

1.7 OVERVIEW OF STUDY

- **Chapter 2** provides background and context to the study documented in this dissertation. A summary of some relevant literature is also presented.
- **Chapter 3** introduces the reader to the QSS toolbox simulation software used in this study. It explains how the original software was updated to use modern components and control strategies. Using these new components a reference vehicle was modelled, which will be used to compare results to the proposed vehicle model. Thereafter the supercapacitor implementation is described. Detailed model operations and diagrams are given for the supercapacitor and its controller. A

new controller block is introduced to manage the power distribution between the Li-ion battery and the supercapacitor. The proposed series HEV is described and modelled using all the updated and newly added components.

- **Chapter 4** presents the numerical and experimental results obtained. Plots are provided to compare results between the reference and proposed models. These results include the use of the ICE, the power distributed between the storage components, battery state of charge and how the battery was utilised. The results are extracted from the QSS toolbox simulations performed, by letting the vehicle models complete both an urban and highway drive cycle.
- **Chapter 5** discusses the results. Positive benefits, as well as the impact it could have on various elements, are discussed based on the results obtained. These include fuel economy, emissions and battery life. A cost analysis is performed in order to determine if the additional energy storage component is a viable option.
- **Chapter 6** concluding remarks are given to provide a complete summary of all the work done and a subjective outcome of the study. Followed by possible future studies.
- **Addendum A** is the final part of the document in which some more screenshots are supplied of the models in the QSS toolbox. These are to provide further context to how the simulation software was used to create the models and how every component is connected.

CHAPTER 2 BACKGROUND AND LITERATURE STUDY

2.1 CHAPTER OVERVIEW

This chapter introduces the basic principles of HEVs and some of its components. Section 2.2 presents the different HEV configurations and why one would be favoured above the other. In Section 2.3 the components and characteristics thereof, that when combined together define an EV or HEV, are discussed. Section 2.4 discusses key aspects of previous studies with similar or relevant information to the work completed and presented in this dissertation. Modified or new components and concepts not introduced in this chapter are presented in Chapter 3.

2.2 TYPES OF HYBRID ELECTRIC VEHICLES

Many of the technologies required to implement an HEV, including ICEs, motors, generators, and power converters, are relatively mature and are widely used in a range of applications. The key challenges to implementing a successful HEV are thus related to power management and energy storage systems.

2.2.1 Series hybrid electric vehicles

Series HEVs use the ICE as a secondary energy source to recharge or support the battery when it reaches a discharged state and is unable to supply power to the electric motor without over-discharging and causing damage. When charging the battery the ICE drives an electric generator which converts the mechanical energy into electric energy. This could in some cases be characterised as an electric vehicle with an ICE as a range extender, but not always. Regardless of whether the ICE is running or not, the only propulsion of the vehicle is by means of the electric motor [15].

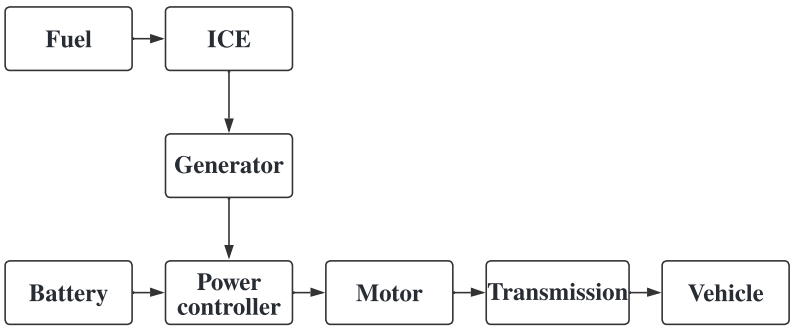

Figure 2.1. Series HEV configuration adapted from [15], with permission.

2.2.2 Parallel hybrid electric vehicles

Parallel HEVs allow for both the electric motor as well as the ICE to propel the vehicle. This means an additional mechanical coupling, like a clutch, is required together with the transmission to accommodate for both machines to work individually or together. In contrast to series HEVs seen as electric vehicles with an ICE range extender. Parallel HEVs are seen as ICE vehicles with an electric motor to be used at low speed or as additional power support when power demand is high [15].

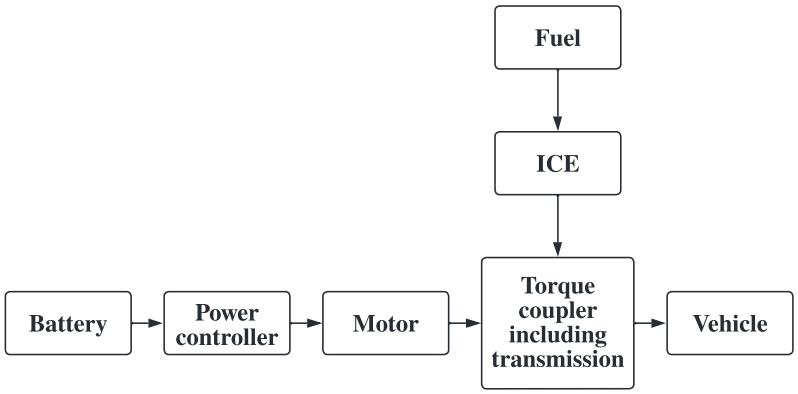

Figure 2.2. Parallel HEV configuration adapted from [15], with permission.

2.2.3 Series-parallel or combined hybrid electric vehicles

These are a combination of features present in both series and parallel HEVs. The configurations are more parallel-oriented. Links of both a mechanical and an electrical nature are present and in some cases, a power split device is also required [15].

2.2.4 Remarks on hybrid electric vehicles

The series HEV configuration makes more sense for this study since it is a closer comparison to electric vehicles. The focus of this study is directed toward reducing emission and fuel consumption while increasing battery life, and not so much on performance. If the study was more focused on performance in terms of acceleration and top speed for example, the parallel HEV might have been a better choice.

2.3 BACKGROUND ON FULL AND HYBRID ELECTRIC VEHICLE COMPONENTS

2.3.1 Batteries

Batteries store energy in a chemical form with many different combinations of chemical components. For example, lead acid batteries use a combination of lead peroxide (PbO_2) and pure sponge-like lead (Pb) for the positive and negative plates respectively, with a fabricated membrane such as an absorbing glass-mat (AGM) separator between them. This is then submerged in a sulphuric acid (H_2SO_4) and water (H_2O) dilution with a 1:3 ratio [16].

Li-ion is a more modern construction without the need for an acid dilution. It is also referred to as a Li-ion battery cell in its singular form and can be conveniently packed together to provide the required voltage and storage capacity due to its compact size and lightweight. The cathode consists of Li-ion compound such as lithium cobalt oxide ($LiCoO_2$) and lithium iron phosphate ($LiFePO_4$), most commonly ($LiFePO_4$). The anode consists of graphite, a molecular structure of carbon. These electrodes are then layered with a separator which ensures only the ions can flow through. The battery further consists of an electrolyte which ensures the ions can flow freely [17].

Li-ion batteries have a significantly higher energy density than lead acid and nickel metal hydrate batteries [18]. Li-ion batteries are capable of up to 10 000 charge and discharge cycles, which is significantly less than supercapacitors or flywheel energy storage systems [18]. These storage devices generally have a power density of up to 340 W/kg and an energy density of up to 200 Wh/kg [18]. Li-ion batteries cost about 10 to 40% of the price ($/kWh) of supercapacitor and flywheel energy storage systems [18].

Some drawbacks of batteries include the limited charging current they are capable of, which increases the time needed to complete a full charge cycle. The low cycle-to-cost ratio means a large financial expense to replace the battery when the usable capacity is no longer acceptable.

2.3.2 Supercapacitors

Supercapacitors are capable of about 1 million charge and discharge cycles, with an efficiency of more than 95%. Supercapacitors have a self-discharge rate of up to 40% per day. Its self-discharge rate is however acceptable since it should charge relatively quickly through regenerative braking. It is also being used as the secondary energy storage system which means it is not critical for the vehicle to start its route [18], [19].

In the last few years, it has appeared that Lithium-based batteries have taken all the spotlight. Lamborghini might have changed things a little with the recent announcement of the Sián FKP 37. This hybrid supercar makes use of a supercapacitor instead of a conventional battery pack, purely for the sake of performance. A supercapacitor has the benefit of being lighter than a battery and charging a lot faster than a battery using regenerative braking. The supercapacitor and 48 V electric motor only add around 34 kg of weight, while being capable of supplying additional power up to 25 kW and torque up to 35 Nm. The supercapacitor has been developed in conjunction with MIT-Italy to have a power density of 2.4 kW/kg and being a low voltage system, a peak current up to 600 A. The addition of this system is claimed to increase acceleration by about 10% [20].

Supercapacitors store their energy electrostatically compared to batteries, where energy is released through redox reactions that occur between electrodes and electrolytes. A supercapacitor is constructed by coating a sheet of aluminium foil on both sides with high-surface-area material. In the case of electrostatic double-layer capacitors (EDLCs), the active material will be activated carbon. Then the two coated sheets are separated with a non-conductive porous film as a separator, to prevent short-circuiting between the positive and negative electrodes. An electrolyte solution is present between each coated sheet and the separator [21], [22].

Supercapacitor storage systems can be a combination of multiple units connected to form a storage bank with the desired specifications [24]. Figure 2.4 presents an image of the supercapacitor module used in this study. Supercapacitors are flexible in terms of sizing and design when trying to achieve

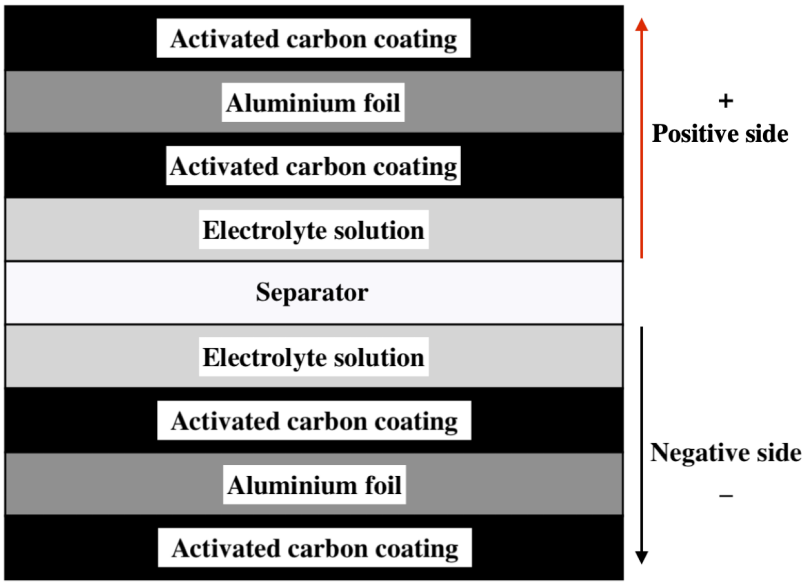

Figure 2.3. Layers of an electric double layer capacitor.

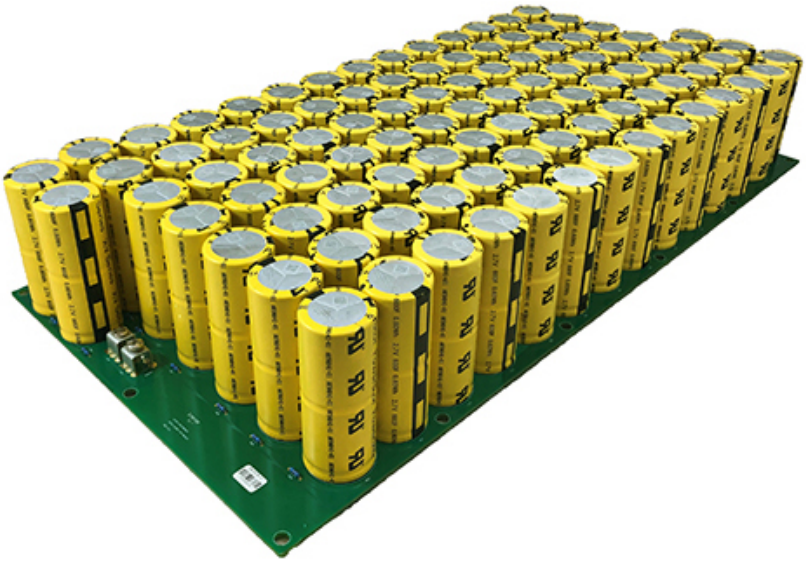

Figure 2.4. Eaton XVM-259R2425-R supercapacitor module [23]. (Requested copyright permission)

a specific power delivery and energy storage capacity. This might also be seen as a drawback since the dimensions increase more than any of the other energy storage systems with the increase in capacity.

2.3.2.1 Flywheel energy storage systems

Even though this study will only be done with the addition of a supercapacitor it is worth noting that it is not the only short-term energy storage system that could be used. A flywheel energy storage system (FESS) is another technology with similar characteristics in terms of high power capability and low energy storage capacity.

This type of energy storage device stores energy in the motion of a flywheel. Energy is stored when the flywheel is sped up (e.g. while braking) and supplied when the flywheel speed is reduced (e.g. during acceleration).

Flywheel energy storage systems are flexible in terms of design and many factors can determine the capability of the system. Factors include the physical dimensions, the quality of mechanical components, and the types of materials used, such as carbon fibre in high speed, high-performance flywheels [19], [25].

2.3.2.2 Supercapacitor used as preferred technology

Due to the mechanical characteristics of a flywheel energy storage system, the biggest limitation could be the integration of such a system. The fact that an additional generator would be needed to implement an electrical influence also makes this a less attractive option. The complexity of integration is especially true in the case of a series HEV configuration. The additional components mechanical and electrical would create unnecessary points susceptible to failure and could render an unreliable vehicle.

The operation and integration of supercapacitors are much simpler and already provide the electrical characteristics required without the need for additional components. The control of power flow is also much more flexible.

2.3.3 Electric motors

As mentioned in Section 2.2, electric motors can be configured to be the main propulsion in series HEVs. Where the motor size is larger, like in full EVs. Smaller motors are more common in parallel

HEVs, since they usually support the ICE with additional power, or allow the vehicle to drive on electric power only at low speed. There are four main motor constructions associated with EVs and HEVs. Switched reluctance motors, brushless direct current (DC) motors, permanent magnet synchronous motors and induction motors.

Switched reluctance motors have the advantage of easy control, robust construction and good torque versus speed characteristics. They do however require different converter topologies and optimisation control strategies. These are required to alleviate some of its drawbacks such as torque ripple. Brushless DC motors are often more associated with full EVs. These motors are very efficient, have a high energy density and are compact in size. Permanent magnet synchronous motors, or sometimes called brushless alternating current (AC) motors, are the closest competitors to induction motors. These motors have high power density, efficiency and good heat dissipation. This motor type is used by many vehicle manufacturers such as Toyota, Nissan and Honda. Induction motors are well established because of the reliability and minimal maintenance they provide. As with DC motors, induction motors have to ability to decouple the flux and torque control, to improve controllability and improve performance. This is known as field-oriented control (FOC) or vector control [26].

2.3.4 Regenerative braking

In the event of braking, a lot of the energy is lost in the form of heat. The heat is generated through the friction caused by the brake pads on the brake disk. Regenerative braking is a concept which used to harvest as much of this energy. This is done by using the same motor used to propel the vehicle as a generator, or using a separate electric generator coupled to the drivetrain. The reverse current is managed by the vehicle's electrical management system and is used to store the recovered energy back into the battery. The amount of braking performed with the electric generator is sometimes controllable and allows the driver to customise the effect regenerative braking has on the driving experience.

According to previous studies, the majority of the total energy efficiency improvements are accounted for with regenerative braking. By harvesting energy the battery charge holds longer, meaning extended battery deployment capabilities. A HEV's fuel efficiency can be improved by up to 40% using this technology [27].

2.4 NOTABLE STUDIES

The concept of a HESS is not new and has been investigated before. HESS technology is not exclusive to new energy vehicles and has been studied in other sustainable energy systems such as solar photovoltaic (PV) systems [28]. A few of the studies related to HEVs will be summarised below. Not many of the other found studies are following the same approach and is considering dissimilar aspects to the study reported in this dissertation.

A study published in 2012 followed a similar, but outdated approach. The goal of that study was to see whether the addition of a supercapacitor to the standard QSS toolbox example of a series HEV would be beneficial for fuel consumption. The results they obtained claimed to have improved the fuel economy by 31.3% [29]. However, that study suffered from several limitations when compared to the study performed and documented in this dissertation. The lacking features are addressed below.

- The supercapacitor was added in a series connected configuration, as opposed to a parallel connection where each storage system can be managed individually.
- The components in the simulation were outdated, such as a lead-acid battery model and a time-based charge controller.
- The model did not have a power management controller to effectively distribute power requirements between the battery and supercapacitor
- This 2012 paper also never discussed the implications the supercapacitor will have on emissions.

A review paper provided some useful insight related to the configuration of the battery and supercapacitor. It was recommended to connect the energy storage systems in parallel to provide individual control. To maximize the performance of the HESS and increase the battery life, a power management system must be implemented [30].

A study focusing on the optimisation of the size of HESS components, revealed that batteries in full EVs are oversized to avoid degradation in high current flow scenarios and to increase travel range. The study introduced an optimisation strategy to determine the optimal size of the battery and supercapacitor to increase the life cycle of the battery. The study used a peak power shaving controller to limit the power delivered by the battery, allowing the supercapacitor to deliver the remaining power required.

The study presented results showing a theoretical battery life increase of about 76% considering only urban driving [31].

In an article published in 2019, it was stated that the ICE can operate at higher efficiency in series HEVs since it is not coupled mechanically to the drivetrain of the vehicle. In the case of a series HEV, the electric motor is the only source of propulsion and the ICE is coupled to an electric generator to charge the battery and provide electrical assistance. The study also stated that recent developments in supercapacitors have provided performance improvements that could make their integration more popular. The study used urban and highway driving environments to simulate the supercapacitor-only HEV model presented. The paper also noted that series HEV configurations are not commonly studied, which is strange since the fuel economy improvements were about 13% higher when compared to the parallel HEV simulated in the same environment [32].

In summary, based on these studies it can be concluded that a parallel configuration should be used to connect the battery and supercapacitor to the proposed vehicle. This would allow better control over each energy storage system individually with the power management controller that has to be designed. It is also evident that series HEVs are not among the common configurations being studied, creating a research gap to investigate it more. Based on [32] it has great potential for fuel economy improvements making it the prefered configuration for this study.

2.5 SUMMARY

HEVs provide a good balance between the desirable characteristics of both EVs and ICE vehicles. An EV is superior when it comes to urban driving environments. Its travelling range increases significantly compared to highway environments and the performance of electric motors providing instant torque makes acceleration a breeze. On the other end ICE vehicles shine in highway driving environments where fuel consumption is significantly less than city driving.

This chapter provided insight into the components which HEVs are comprised of. A few notable studies with relevant facts and guidance to this study were summarised. These included recommendations on how to combine multiple energy storage systems and how they can be controlled.

CHAPTER 3 IMPLEMENTATION AND SIMULATION

3.1 CHAPTER OVERVIEW

The chapter covers all the aspects of the modelling and simulations performed in this study. The different commonly used simulation packages are presented together with the motivation of why the QSS toolbox was considered above the other options. A brief introduction is presented regarding the QSS toolbox, and an example was given of how a typical model would be designed and configured. Updated models, as well as new models, such as the battery, its controller, and the power management controller, are discussed. The configurations of the complete reference vehicle and the proposed vehicle are discussed.

3.2 SOFTWARE

A few different software packages that have HEV simulation capabilities have been considered. The main focus was a program that could be easily modified and accept additional models and designs.

3.2.1 Software selection

The first option was Advisor Advanced Vehicle Simulator which is extremely detailed and as the name suggests is very advanced compared to other Matlab-based vehicle simulators. The drawback with simulation software of this complexity is the restrictions to adding additional components and models.

The second package investigated was the HEV Series-Parallel Model developed by Steve Miller and is

available on the Matlab file exchange. The HEV Series-Parallel Model is not as advanced in terms of features compared to Advisor Advanced Vehicle Simulator but is a highly detailed series-parallel vehicle configuration. The drawback with this model is the compatibility with additional components which are not as detailed to comply with the rest of the model. This would become too complex for the outcome requirements and expectations set for this study.

The judicious option was the QuasiStatic Simulation Toolbox (QSS) developed by ETH university in Zürich [33]. This software was constructed and developed in a way which made it more compatible with the requirements of this study when compared to the other options. The software package is freely available and runs within MATLAB and Simulink environments. All the vehicle components are realised as function blocks and are effectively combined to create the desired vehicle configuration. This simulation package was chosen because of the flexibility it provides to make modifications to component function blocks or add additional components, which were required in this case.

The computer used is loaded with Windows 10 Pro operating system, with MATLAB version R2019b update 8 Student License. Computer specifications are as follows: Intel i7-8700 processor, 16 GB DDR4 2666 MHz memory, NVIDIA GeForce GTX 1070 Ti graphics card with 8 GB video memory. Simulation runtime is approximately 6 s.

3.2.2 QSS toolbox overview

The QSS method is a simulation method which determines the required results in a reverse process. This means that all the input values are required to be known before the process can begin. In a case such as this, a drive cycle is used to simulate a virtual path the vehicle must follow, meeting the aforementioned requirement. The calculations are executed at fixed time intervals of 1 s each until the end of the drive cycle is reached. The QSS approach is not as mathematically complex to model as a dynamic simulation approach, and is thus much easier to design components to be compatible with each other. This ensures components are able to be used in various configurations. This method is capable of simulating very complex models where power flow is predominant, such as vehicles. Making this a good platform to use to optimise and minimise key aspects of this study such as fuel consumption [15]. The QSS toolbox is a tool developed to simulate vehicles of any configuration, such as ICE only, HEV (parallel, series or a combination of both) or full EVs. What makes this software unique is that it works with function blocks for each of the components present in the desired

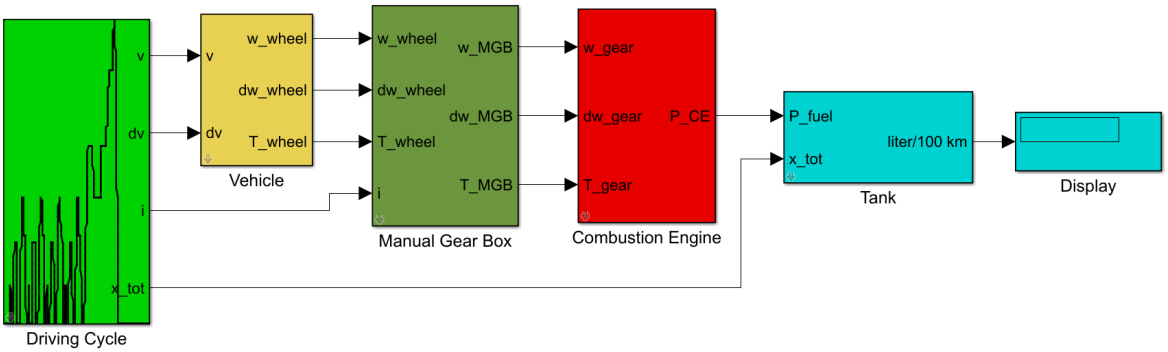

Figure 3.1. Example model of an ICE vehicle model in QSS toolbox.

configuration. This concept makes it much more compatible to add new or redesigned components to the model. In other software models previously mentioned, it is believed to be a more integrated system between the components which would lead to a whole redesign of the model to make a modification possible. This is undesired and there the QSS toolbox is confidently a better choice for the scope of this study.

In Figure 3.1 the different function blocks can be observed. The visual aspect of designing a HEV model in the simulation software is done using Simulink. Figure 3.1 shows a sample model of a vehicle which has a ICE as its only source of power. The model starts with the drive cycle followed by the vehicle parameters, gearbox and combustion engine blocks. The final part of the model labelled the tank, determines the amount of fuel used based on the consumed energy throughout the drive cycle and displays the fuel consumption in L/100 km [1].

3.2.3 Drive cycles

A drive cycle refers to the virtual route that the modelled vehicle follows with various acceleration and deceleration profiles. A drive cycle consists of a data file containing the following four vectors:

- $\overrightarrow{V\_Z}$ = speed vector
- $\overrightarrow{T\_Z}$ = time vector
- $\overrightarrow{D\_Z}$ = acceleration vector
- $\overrightarrow{G\_Z}$ = gear number

[1] Throughout the document L/100 km refers to litres per 100 km

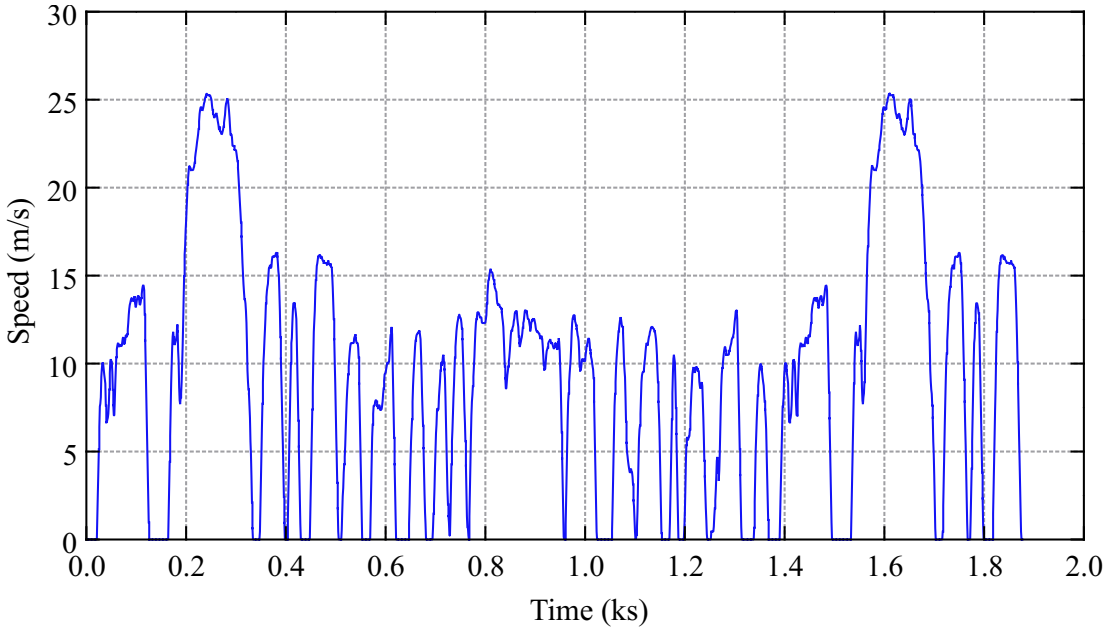

Figure 3.2. Urban drive cycle FTP-75 profile [34].

These vectors are used as the first input values to the model during the simulation process. The drive cycles are chosen using the drop-down menu in the window when double-clicking on the drive cycle block on the Simulink modelling page.

Generally, vehicle fuel consumption is claimed as city, highway and combined values. In this dissertation the combined fuel consumption is defined as the equally weighted average between city and highway fuel consumption. The chosen city drive cycle is the FTP-75, which is also known as the EPA75. The highway route chosen is the Highway Fuel Economy Test (HWFET), labelled as the FTP-Highway drive cycle. These drive cycles are recognised as testing schedules by the United States Environmental Protection Agency (EPA).

The FTP-75 consists of the EPA Urban Dynamometer Driving Schedule (UDDS) and is followed by a repeat of the first 505 s of the same cycle. This gives the urban drive cycle a total distance of 17.77 km completed in 1 877 s. The speed plot over time can be observed in Figure 3.2. The acceleration and deceleration is very deliberate and frequent throughout the drive cycle as expected in an urban driving environment. It can also be seen that the maximum speed was about 25 m/s (90 km/h) for very short periods of time.

The FTP-Highway drive cycle consist of a 16.49 km route, that would take the vehicle 765 s to

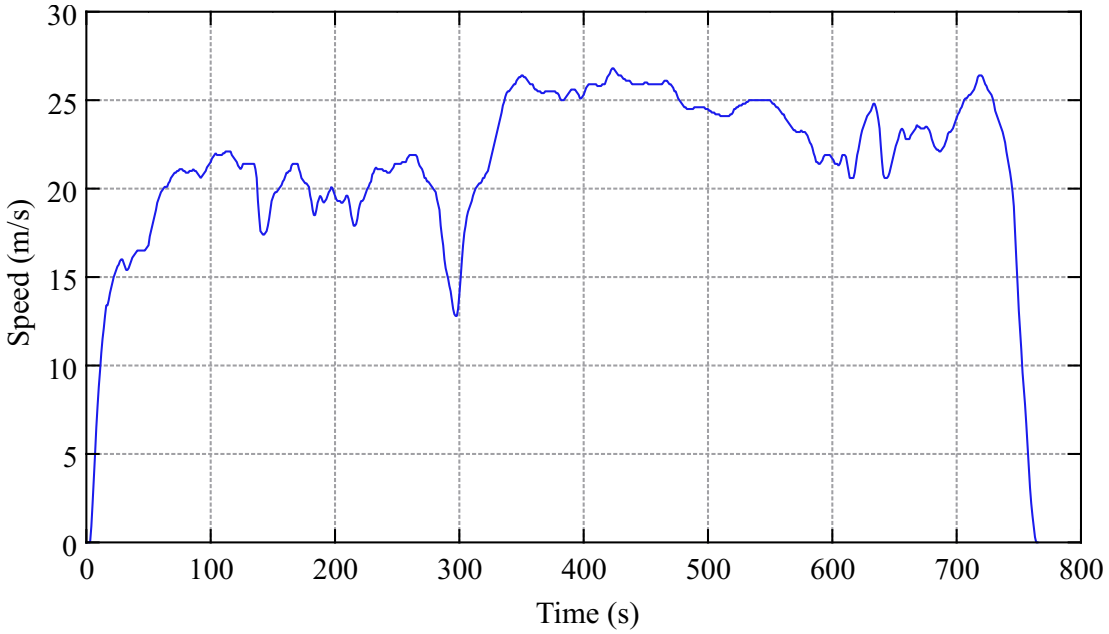

Figure 3.3. Highway drive cycle FTP-Highway profile [34].

complete. Compared with the FTP-75 drive cycle, the route completion time is 18.5 minutes faster for a 1.28 km shorter distance. The longer sustained high-speed values are also a clear indication that Figure 3.3 resembles a highway environment.

3.2.4 Updated battery model

The battery model in the original version of the QSS toolbox is using lead-acid type batteries. This had to be updated to simulate the more commonly used Li-ion type battery. Li-ion batteries are designed with combinations of series and parallel cells usually around 3.7 V nominal per cell. The battery bank is then constructed with cells in series up to the desired voltage, and then those series combinations are repeatedly connected in parallel to reach the required Ah capacity. For simplicity the battery capacity can be specified, thus eliminating the need for calculation of the parallel cells. The number of series cells cannot be eliminated in the same way since the SOC and voltage relationship data is for a single cell. A new mask was also created in the graphical user interface (GUI) of the model design page.

The mask interface makes it easy to change any component's parameters on the Simulink modelling page. Figure 3.4 can be accessed by double-clicking on the battery block of the vehicle model. It gives the option to change the initial charge of the battery with a value of 1 being 100%. The voltage of the

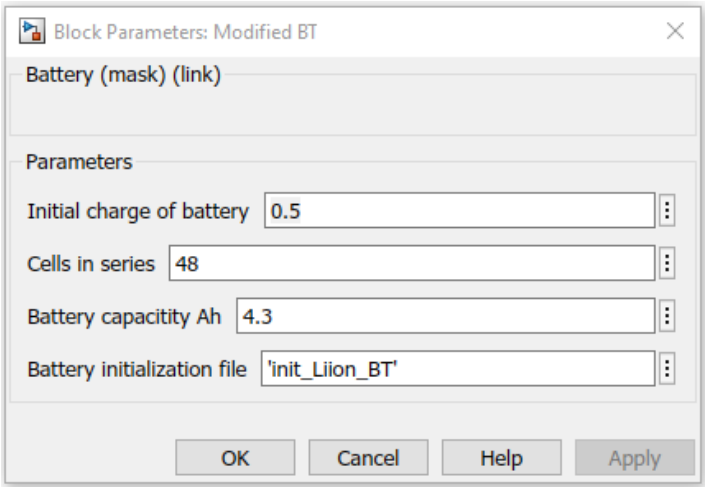

Figure 3.4. Battery mask GUI interface.

battery can be changed by changing the number of cells connected in series with a single cell being 3.7 V. The battery capacity measured in Ampere-hour (Ah) can also be changed.

The battery initialisation file is a .m file containing the data of a commercially available Li-ion cell. The data is a series of voltage values of the battery at specific states of charge. This data is then used to interpolate the voltage and state of charge of the battery during simulation. The battery cell being used is the Saft MP 176065 HD Integration Rechargeable Li-ion battery [35]. Table 3.1 shows the battery charge percentage with its correlated voltage used for interpolation.

Table 3.1. State of charge (SOC) and correlating voltage of single cell Li-ion battery.

SOC (%)	0	10	20	30	40	50	60	70	80	90	100
Voltage (V)	3.20	3.40	3.50	3.60	3.62	3.65	3.70	3.74	3.82	3.90	4.00

The Li-ion battery block receives the required power at each instance of the drive cycle. The first part of the function block calculates the current required by the vehicle based on the voltage that was fed back from the previous instance. Thereafter the new state of charge is determined based on the energy consumed. The new voltage is then calculated relative to the number of cells connected in series, whereafter the new voltage value is looped back to be used in the following instance. Figure 3.5 illustrates the function performed inside the battery model. This process is repeated for every second in the drive cycle. The voltage and state of charge are output from the battery block to be used as input in the next block in the vehicle model.

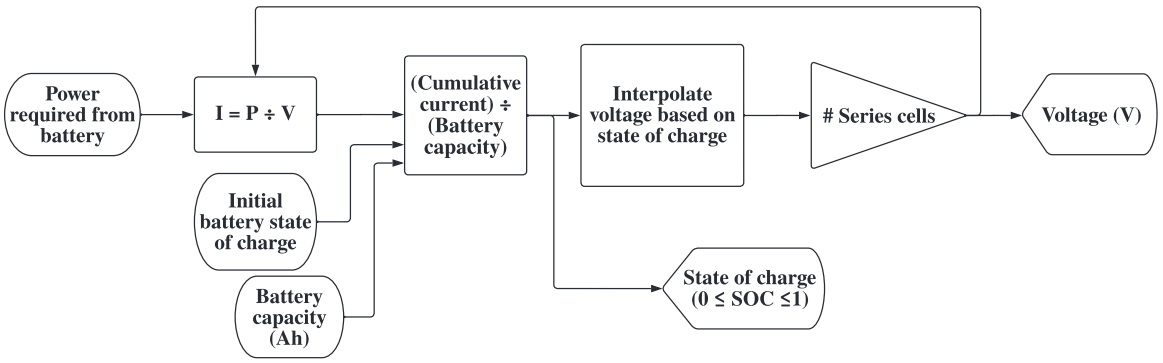

Figure 3.5. Battery model.

3.2.5 Updated battery controller

It was observed that the original battery controller was not a flexible model, meaning it used a fixed time for charging. As soon as the battery reached a set discharge value it would charge the battery for the predefined time and would not stop charging before that time is reached. This caused problems, especially when the drive cycle has long periods of regenerative charging. The battery would charge beyond full capacity and cause the simulation to reach an error and abort. Alternatively, the power requirements of the vehicle are high during the battery charge period, causing the battery to unsuccessfully reach a fully charged state.

A dynamic model had to be designed to ensure the battery would charge to full capacity in any circumstance. The following points had to be considered during the battery controller design.

- The battery discharge curve is determined by the number of power it needs to supply the electric motor.
- The power requirements are based on the drive cycle given to the model.
- The charge operation of the controller should be able to compensate for the behaviour of the additional energy source, which in this case is the supercapacitor.
- The new controller must accept a lower state of charge values since Li-ion batteries are capable of deeper discharge than lead-acid batteries.

The original battery charge controller managed a ramp up and ramp down of the ICE running speed. The ICE drives the electric generator when charging the battery. This provides a rather gradual increase

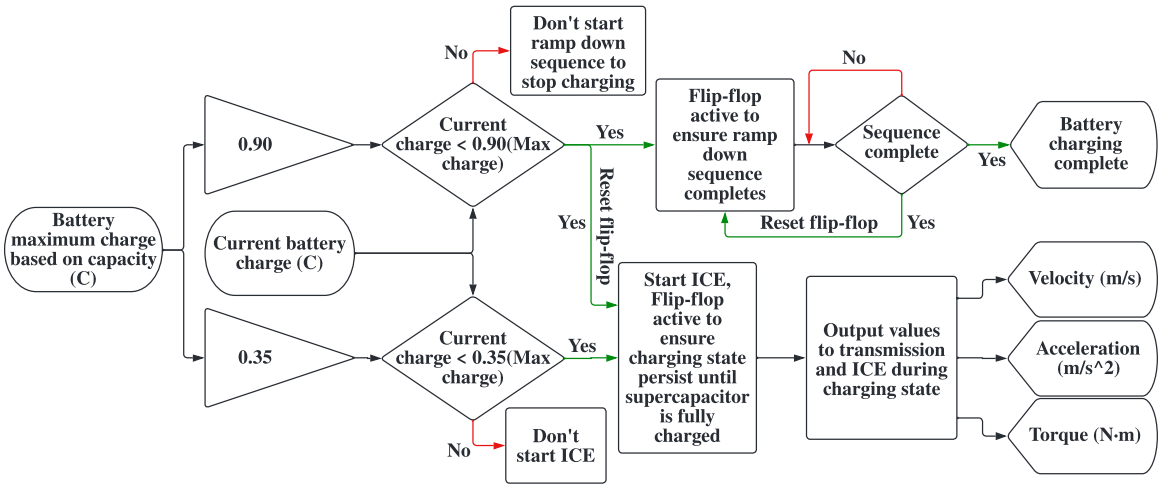

Figure 3.6. Battery controller diagram.

and decrease of charge current. This also protects the battery from a potentially damaging inrush or surge current. Since the original controller was using a predefined period to charge the battery, the ramp-down period was triggered based on a counter and not based on the battery's state of charge. Therefore, the ramp up and ramp down functions had to be redesigned. The redesigned functions now continuously monitor the state of charge of the battery. This ensures the controller operates within the battery's limits regardless of the drive cycle the vehicle is simulated with.

The battery's real-time charge (C) and capacity (Ah) is received as input to the battery controller block. The battery controller firstly calculates the maximum and minimum charge (C) constraints based on the Li-ion battery's set capacity (Ah). These constraints then act as the maximum and minimum state of charge the battery is allowed to operate in. For the sake of battery longevity, the choice was made to set these SOC maximum and minimum constraints as 98% and 20% respectively. The ramp-up sequence to charge the battery will start as soon as the battery discharges below 35% and the ramp-down sequence to stop charging will start at 90%.

As seen in Figure 3.6 the battery controller is responsible for the output of velocity, acceleration and torque values. These values are supplied to the transmission and ICE for those blocks to determine if the ICE would need to be utilised for additional power or to charge the battery. The above-mentioned outputs supply the start and stop sequence of the ICE. The ramp up and ramp down values of the ICE are contained in lookup tables, and are called over a 28 second period. About halfway through the increase of engine speed, the electric generator starts to supply a charging current to the battery. A

small dip in power delivery by the ICE is noticeable in Figure 4.8 and 4.9.

3.2.6 Reference vehicle

It was decided to use a reference vehicle in order to compare the results with a real-world vehicle. The vehicle chosen was a Toyota Yaris Hybrid. This vehicle is a small hatchback using hybrid technology. According to a magazine article published online in 2021, hatchback vehicle types are the most common among United Kingdom (UK) motorists [36]. Making the Yaris model a prime candidate to be used as a reference vehicle.

The specifications such as the engine size measured in cubic centimetres (cc), weight (kg), battery voltage (V) and capacity (Ah) are used. This would allow for a model to be created in the software very close to the Toyota Yaris Hybrid. Simulating this model should obtain realistic results to be used for comparisons to the proposed model with an additional supercapacitor.

The vehicle data sheet was obtained from an official Toyota website [37]. Table 3.2 contains a summary of the relevant parameters. These parameters are used to redefine the model in the QSS toolbox as the reference model for the rest of the study. The vehicle mass of 1 200 kg is determined by the kerb weight of 1130 kg stated in the specifications and a driver of 70 kg. Additionally, the specifications sheet also stated that the claimed fuel consumption of the vehicle is 3.3 L/100 km [37]. It is assumed that this is the combined fuel consumption, meaning the equally weighted average of the fuel consumption between city and highway driving. It is expected that the simulated series HEV model with these specifications should achieve a combined fuel consumption within at least 5% of the actual vehicle. This would confirm that the simulations are acceptably realistic and any comparisons made will be relevant.

It is also important to have the emissions figures stated for the Toyota Yaris Hybrid [39]. The values will enable the ability to calculate the reduction of emissions as a result of better fuel economy. The emissions summarised in Table 3.4 are relevant and remain a baseline since no altercation or modifications will be made to the ICE itself. The addition of a supercapacitor to the model will only alter the way in which the ICE is utilised.

Table 3.3. Emissions as stated by the specifications sheet [39].

Type	Value
Carbon dioxide (CO_2)	112 g/km
Carbon monoxide (CO)	148.7 mg/km
Total hydrocarbon content (THC)	24.6 mg/km
Nitrogen oxide (NO_x)	9.5 mg/km

The raw values from the specification sheet that are listed in Table 3.3 are presented in g/km or mg/km. Since the length (km) of the drive cycles is known and the simulation returns the fuel consumption in L/100 km, it would be easy to determine the amount of fuel used in litres (L). To calculate the number of litres used in simulation, (3.1) is used.

$$\text{Fuel used (L)} = \text{Fuel consumption (L/100 km)} \times \text{Distance (km)} \tag{3.1}$$

Additionally, the emissions from Table 3.3 are recalculated since the fuel consumed becomes the appropriate variable to determine the emissions produced, especially after the supercapacitor is added. The values are recalculated using (3.2) to (3.5).

Table 3.2. List of vehicle parameters.

Parameter	Value
Vehicle mass	1 200 kg [37]
Combustion engine size	1.5 L (1 490 cc) [37]
Number of battery cells in series (3.7 V each)	48 (177.6 V total) [38]
Initial SOC of battery	50%
Battery capacity	4.3 Ah [39]
Battery operating range	20% to 98%

$$\text{Carbon dioxide } (CO_2)\ (\text{kg/L}) = \frac{\text{Rate of } CO_2 \text{ emission (g/km)}}{\text{Fuel consumption (L/100 km)}} \times 0.1 \tag{3.2}$$

$$\text{Carbon monoxide (CO) (g/L)} = \frac{\text{Rate of CO emission (mg/km)}}{\text{Fuel consumption (L/100 km)}} \times 0.1 \tag{3.3}$$

$$\text{Total hydrocarbon content (THC) (mg/L)} = \frac{\text{Rate of THC emission (mg/km)}}{\text{Fuel consumption (L/100 km)}} \tag{3.4}$$

$$\text{Nitrogen oxide } (NO_x)\ (\text{mg/L}) = \frac{\text{Rate of } NO_x \text{ emission (mg/km)}}{\text{Fuel consumption (L/100 km)}} \tag{3.5}$$

After the simulated fuel consumed is calculated using (3.1), Table 3.4 is used to calculate the amount of each of the gasses emitted.

Table 3.4. Baseline emissions produced by vehicle.

Type	Value
Carbon dioxide (CO_2)	3.4 kg/L
Carbon monoxide (CO)	4.5 g/L
Total hydrocarbon content (THC)	745.5 mg/L
Nitrogen oxide (NO_x)	287.9 mg/L

The real-world Toyota Yaris Vehicle is not constructed in a series HEV configuration, but rather in a parallel HEV configuration. Even though, this study uses a different configuration it is important to note that this is a reference vehicle within the simulation environment to compare the proposed model with. The proposed vehicle will not be directly compared to the Toyota Yaris Hybrid, but to the model that presented nearly identical performance during simulation. Ensuring that the results obtained within this study do have merit compared to real-world HEVs.

Figure 3.7 is a simplified representation of how the series HEV model is designed in the QSS toolbox. The model has the same function blocks and is connected in the same flow pattern. The difference is that there are multiple connections between the blocks that contain different variables, in contrast

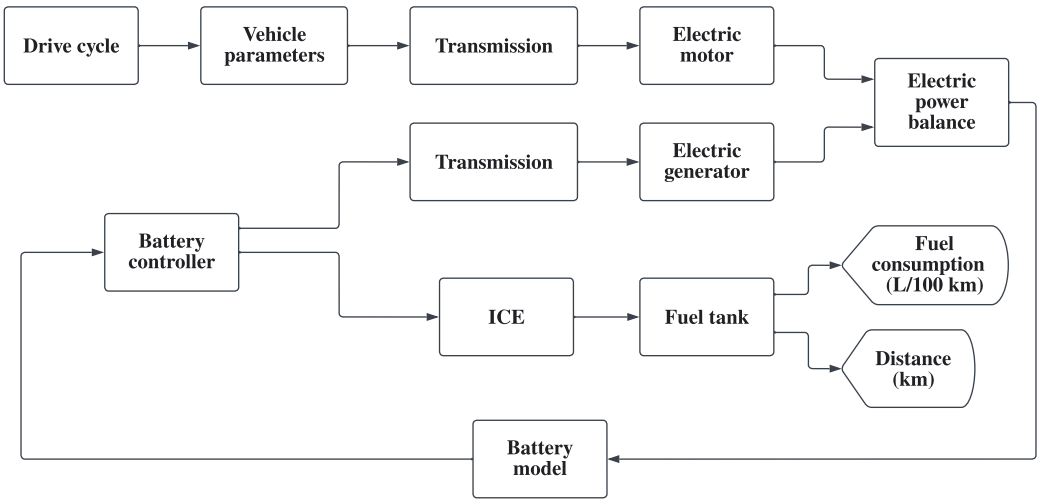

Figure 3.7. Simplified reference series HEV configuration.

to only the single connections in Figure 3.7. A screenshot of the complete reference model designed with the QSS toolbox in Simulink can be seen as Figure A.2 in the Addendum. The aforementioned figure is the final vehicle with the additional and redesigned components added, not the reference vehicle.

3.3 SUPERCAPACITOR IMPLEMENTATION

3.3.1 Overview

This section provides all the details about the experiment of which the aim was to increase battery longevity and the overall efficiency of the HEV, which entails the reduction of the fuel economy and emissions. The experiment involves adding an additional short-term energy storage system. Short-term suggests that the additional storage system must be much smaller in energy storage capacity than the Li-ion battery. The battery remains the primary energy storage, but the intent will be to reduce the load on the battery during instances where power demand is high. This will potentially increase vehicle range as well as battery service life.

The two energy storage components are controlled individually and therefore made sense to model them in a parallel configuration. The implementation was done using the configuration illustrated in Figure 3.8. The supercapacitor model and supercapacitor controller model will be presented in this section. A new controller will also be introduced to manage the bidirectional power requirements of

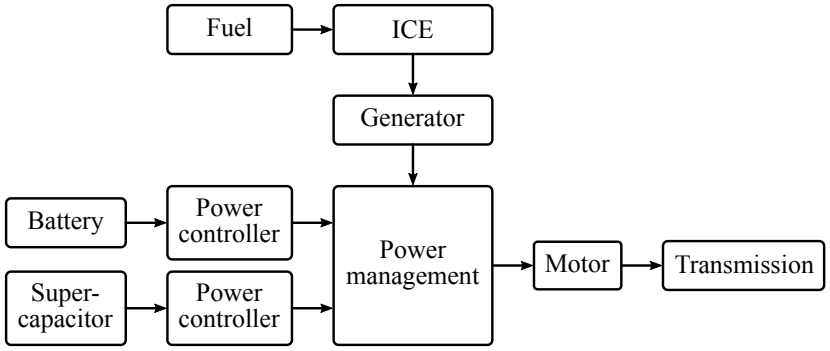

Figure 3.8. The proposed series HEV configuration with a supercapacitor.

the two energy storage systems.

3.3.2 Supercapacitor model

It was decided that the supercapacitor should be relatively small compared to the energy storage capability of the Li-ion battery. The energy storing capacity of the supercapacitor was specified to be about 5% of the size of the battery. It was also important to choose a supercapacitor that is commercially available, to eliminate the chance of the specifications used in simulations being unrealistic. The supercapacitor module chosen utilises an electric double layer cpacitor (EDLC) construction, an image of the module can be observed as Figure 2.4. It has a capacity of 4.17 F and a maximum voltage of 259.2 V [23]. The important factor to consider with a supercapacitor is the operating voltage. The usable voltage of the supercapacitor, in this case, is between 154 V and roughly 5% below maximum voltage to avoid over-voltage. The minimum voltage is defined by the minimum voltage of the battery. The battery's minimum cell voltage is 3.2 V and with 48 cells in series, this equates to 153.6 V.

Table 3.5 summarises the parameters of the supercapacitor and power management controller that had been added to the system. The supercapacitor is capable of storing 38.9 Wh of energy, which is only about 5% compared to the Li-ion battery's 763.7 Wh. This was deemed a reasonable design choice to ensure that the cost compared to the functionality ratio is not ambitious since the supercapacitor has a defined role as a supplemental short-term energy storage solution.

The price of the supercapacitor module at the time of writing in July 2022 was USD 2 563.17 per unit on the Avnet online store [40]. The buyback period and cost compared to benefit will be discussed in Section 5.

Table 3.5. List of supercapacitor parameters.

Parameter	Value
Supercapacitor capacity	4.17 F [23]
Supercapacitor voltage	259.2 V [23]
Supercapacitor price	USD 2 563.17 [40]
Initial SOC of supercapacitor	95%
Supercapacitor operating range	60% to 95%

The same as with the updated battery model and many other components the parameters in Table 3.5 are inserted into the simulation workspace using a mask in the GUI.

The equivalent circuit used to model the supercapacitor in the QSS toolbox consists of a capacitive and resistive component. Thus the current flow equation has been derived and can be found in the QSS toolbox manual as [33]

$$I_{sc} = \frac{-\frac{Q_{sc}}{C_{sc}} + \sqrt{\left(\frac{Q_{sc}}{C_{sc}}\right)^2 - 4P_{sc} \cdot R_{sc}}}{2 \cdot R_{sc}}. \tag{3.6}$$

The variables in (3.6) are defined as

I_{sc} is the instantaneous current flowing through the supercapacitor,

Q_{sc} is the instantaneous charge held by the supercapacitor,

C_{sc} is the capacity of the supercapacitor,

P_{sc} is the power flowing from and to the supercapacitor,

R_{sc} is the internal resistance of the supercapacitor.

Equation (3.6) is inserted into the model in the QSS toolbox as seen in Figure 3.9. This makes it possible for the model to determine the instantaneous charge and voltage correlating to the current determined from the power transferred from and to the supercapacitor. The connection points create a feedback loop, to ensure the calculations are made accurately and dynamically.

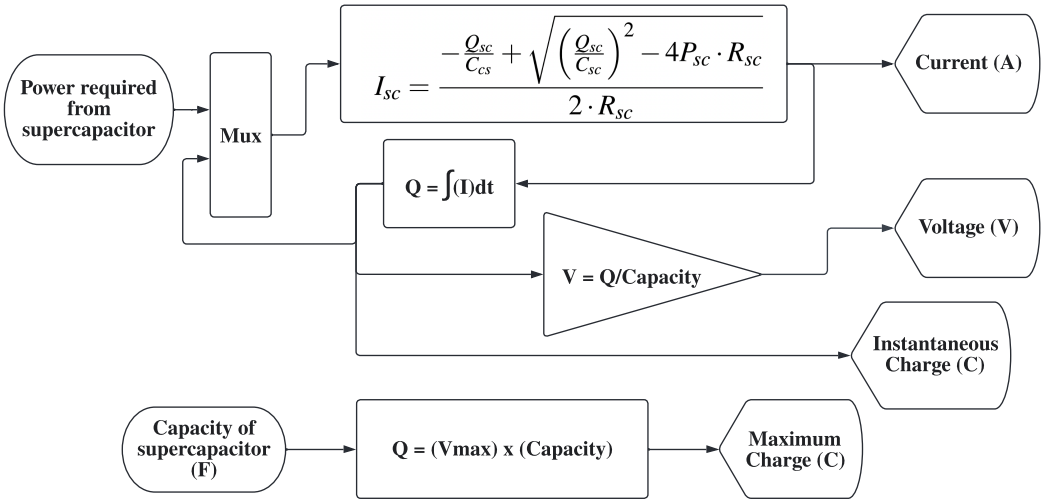

Figure 3.9. Supercapacitor model.

The initial value of the parameter Q_{sc} is defined by (3.7) and C_{sc} and R_{sc} by (3.8) and (3.9) respectively. C_{sc} and R_{sc} are constants retrieved from the supercapacitor datasheet [23]. Whereas parameters I_{sc} and P_{sc} are determined for every second of the simulation based on the inputs from the drive cycle.

$$\begin{aligned} Q_{sc} &= C_{sc} \times V_{sc} \\ &= 4.17 \times 259.2 \\ &= 1080.86\ C \end{aligned} \tag{3.7}$$

$$C_{sc} = 4.17\ F \tag{3.8}$$

$$R_{sc} = 0.31\ \Omega \tag{3.9}$$

An additional function was added to the supercapacitor block to calculate the maximum charge of the supercapacitor by using the maximum voltage and the preset supercapacitor capacity, formulated by (3.7). This value is transferred to the power management controller. This added function ensures that by simply changing the supercapacitor's capacity, the rest of the system can adjust accordingly. Previously when making adjustments using the original QSS model, the rest of the system had to be modified manually to account for those adjustments. Making this approach much more convenient.

3.3.3 Supercapacitor controller

Since the QSS toolbox did not have a supercapacitor controller, the updated battery controller from Section 3.2.5 was a good starting point. The supercapacitor controller is operationally very similar to the battery controller. It manages the flow of current into and out of the supercapacitor. It ensures that the supercapacitor is always within its usable operating voltage, avoiding overcharging or discharging beyond a usable voltage. Therefore the operating range of the battery will be between 60% and 95% of its capacity.

The ramp-up and ramp-down sequence presented in Section 3.2.5 is a nice solution to avoid surge current and will be implemented in the supercapacitor controller as well. The supercapacitor controller uses a time-independent approach to ensure that the supercapacitor is always sufficiently charged before the charging stops.

The integration of the supercapacitor and its controller is done in a parallel configuration to the battery and its controller, as seen in Figures 3.8 and 3.12. This makes it easier to control the flow of power between the energy storage systems. The supercapacitor and battery operate completely independently but have the ability to combine their power delivery. The velocity, acceleration and torque outputs of this block are connected to summation functions with the same corresponding outputs from the battery controller. The results of these summations are then connected to the ICE and transmission blocks.

The charge and discharge states of these two energy storage system are determined by the power management controller presented in Section 3.3.4.

3.3.4 Power management controller

To accommodate a second energy-storage system, the way the power is distributed needed to be redesigned compared to the original QSS model. Supercapacitors are capable of delivering large amounts of power, but for a short amount of time. The power distribution controller was designed in a power flow structure that is representative of power peak shaving. This ensures during instances where the power required reaches above a predetermined value, the load would be split between the battery and secondary energy-storage system.

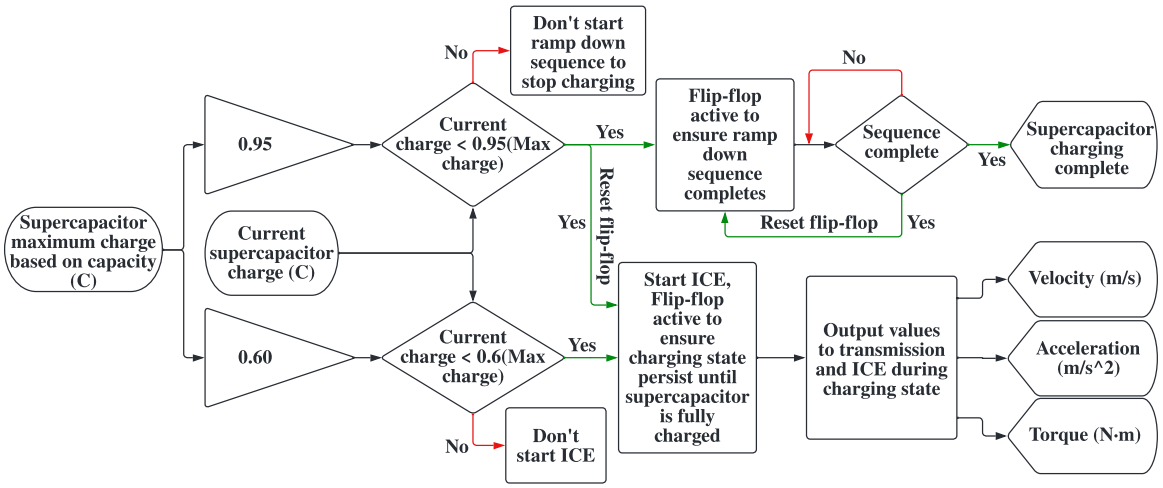

Figure 3.10. Supercapacitor controller diagram.

This rule-based strategy of power peak shaving is commonly used in energy optimisation, as observed in a full EV study where a HESS was present [31]. It could also be referred to as a high-pass filter/low-pass filter (HPF/LPF) approach [28]. The way this controller works is logical and descriptive and since this study was not purely focussed on the control component of the HEV simulation it was decided to use a comprehensible rather than a complex control strategy. Where the sum of the two outputs must be equal to the total power required. The battery will cover the lower part of the power requirements up to a specified cutoff. The supercapacitor will handle the upper part of the power peak. If there is no peak above the cutoff the supercapacitor will not be used.

The controller designed for this study will minimise the occurrence of peaking current drawn from the battery. A smoother battery discharge profile can be expected since the supercapacitor will absorb any power spikes. This has positive impacts such as reduced strain on the battery cells and lower overall temperature. Most importantly, it will increase the cycle time and the number of cycles of the battery.

In Figure 3.11, a flowchart is presented to provide insight into how the power is managed by the controller during charging and discharging states. A screenshot of the actual model designed in the QSS toolbox can be observed in Figure A.3 in the Addendum at the end of this document.

The controller in this simulation was set to perform peak shaving when the power required was above 7.5 kW. The controller also confirms that the supercapacitor has enough charge to handle the

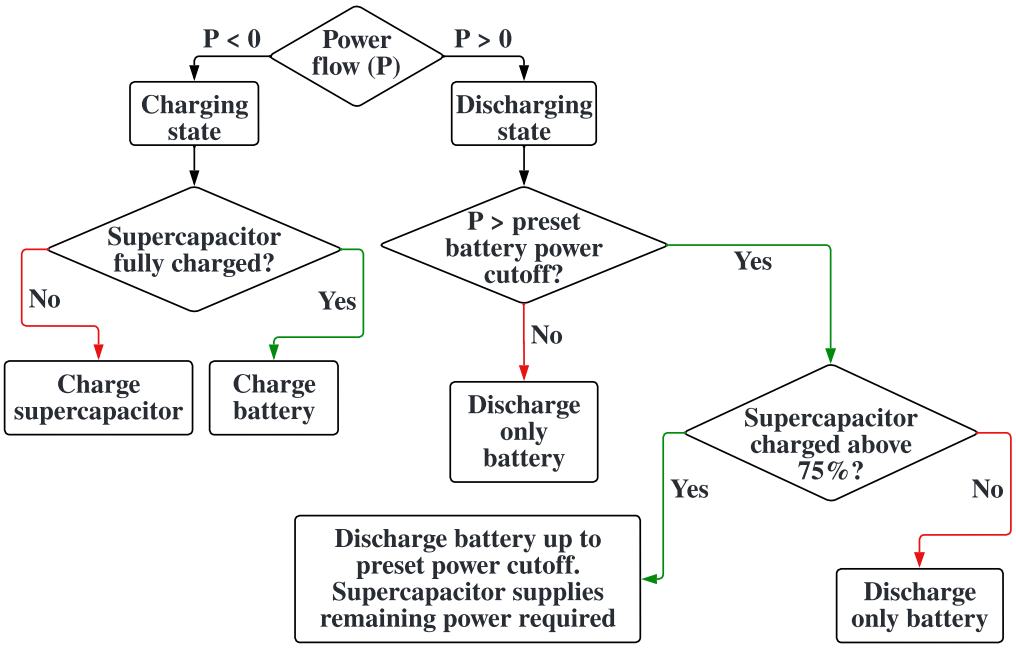

Figure 3.11. Power management controller.

power required. Ensuring the supercapacitor is not discharged below 60% where the voltage becomes unusable.

The charging priority is also managed by this controller. It will give the supercapacitor the first priority to ensure it is ready to deliver power as much as possible to reduce the load from the battery. If the supercapacitor is already fully charged, the battery will be charged during a negative current instance, which could be regeneration or generation from the combustion engine.

In Algorithm 1 the operation of the power management controller is described. From lines 1 to 13, the distribution of power delivery is handled. Lines 14 to 20 describe the charging states when energy is harvested.

3.3.5 Proposed vehicle model with supercapacitor

The components specified in Sections 3.2.4 to 3.2.6 and 3.3.2 to 3.3.4 were combined together to construct the proposed vehicle model. A simplified illustration of the configuration of the new model can be observed in Figure 3.8. The diagram shows that the battery and its controller now operate together with the supercapacitor and its controller in a parallel configuration. The power flow of these

Algorithm 1 : Determining the power delivery and charging scheme of the HESS.

if $P_{required} > 0$ **then**
  $P_{shaved} = P_{required} - P_{preset\ value\ where\ peak\ shaving\ occurs}$.
  if $P_{shaved} > 0$ **then**
    if $Q_{sc} > 0.75 \cdot Q_{sc\_max}$ **then**
      use the battery and supercapacitor to supply power.
    else if $Q_{sc} = 0$ **then**
      HESS is being charged.
    else
      supercapacitor not sufficiently charged, use battery only.
    end if
  else
    no power shaving necessary, use battery only
  end if
else if $Q_{sc} > 0.90 \cdot Q_{sc\_max}$ **then**
  supercapacitor is sufficiently charged, charge the battery.
else if $Q_{sc} = 0$ **then**
  power is being consumed from the HESS.
else
  supercapacitor has charging priority until it is sufficiently charged.
end if

energy storage systems is controlled by the power management controller. The power management controller splits the energy consumption between the energy storage systems conditionally as discussed in Section 3.3.4. The power is then transferred to the motor whereafter the rest of the system operates as it did with the original series HEV model.

The complete model can also be observed in Figure A.4 which is a screenshot attached in the Addendum. All the blocks that are not filled with colour are newly designed or updated components implemented in this study. It is important to remember that the QSS method is a reverse simulation method. So even though the blocks are connected in a forward direction the simulation is actually performing its calculation in the opposite direction as what would be performed by a dynamic model.

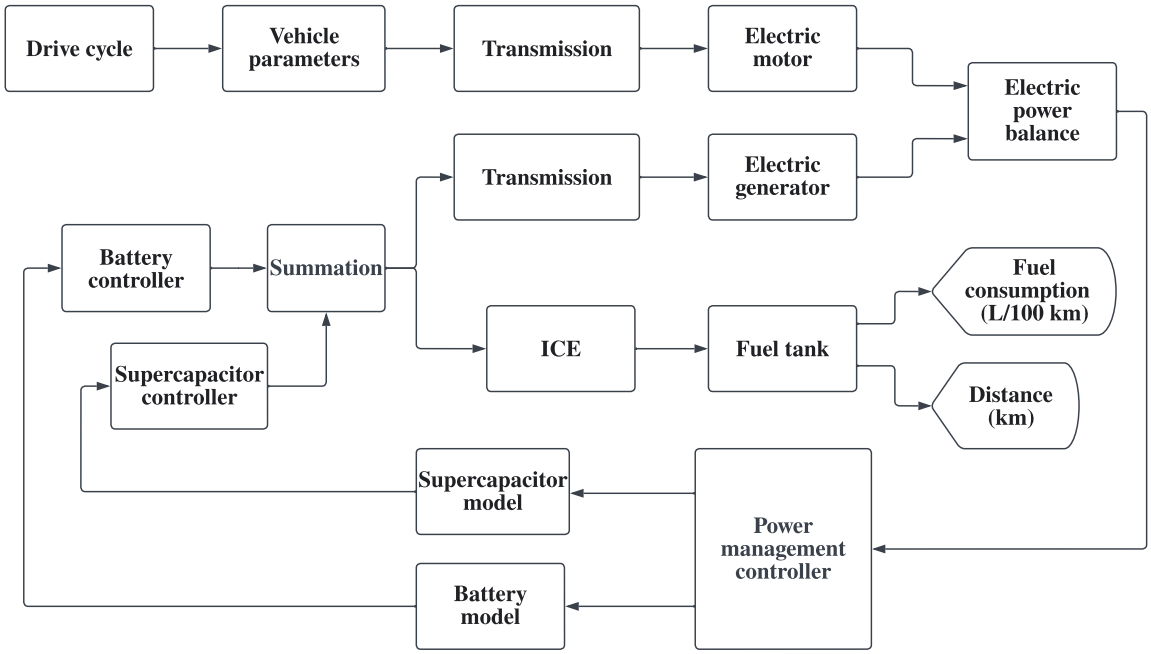

Figure 3.12. Illustration of model in proposed HEV configuration.

3.4 SUMMARY

In this section, the essential components of HEVs and their models were discussed. A reference vehicle and a proposed vehicle configuration were modelled. It was decided to model the reference vehicle based on the specifications of a Toyota Yaris Hybrid. Ensuring the results obtained are relevant and have a reference to real-world performance. The proposed vehicle contained the updated components as well as the additional supercapacitor and power management controller. The proposed system is the result of the recommendations followed by other studies mentioned in Section 2.4. It was decided that the drive cycles used in this study should resemble both a highway and an urban environment to derive an accurate combined result. 6

CHAPTER 4 RESULTS

4.1 CHAPTER OVERVIEW

This section provides the results and comparison of the vehicles with and without the additional supercapacitor. The aspects consider include the battery power usage, power distribution between the battery and supercapacitor, engine utilisation, battery SOC, fuel consumption and emissions. All these factors were considered for both the urban and highway driving cycles. The initial and constant parameter values can be observed in Addendum A at Section A.1.

4.2 POWER REQUIREMENTS

The following results display the power requirements based on the speed profile for the city and highway drive cycles respectively. The power requirements plots are important because it will be used in the subsections of results that follow to show how the battery and supercapacitor behaves. For each drive cycle this power requirements profile remains fixed, independently of the source or multiple sources that would supply the power.

It is evident that in the city drive cycle shown in Figure 4.1 that the power and speed is fluctuating frequently. This is due to the vehicle accelerating and decelerating. Just before the speed increases there is a spike in power required in order to get the vehicle to accelerate. During deceleration the power becomes a negative value, indicating the harvesting of energy due to regenerative braking.

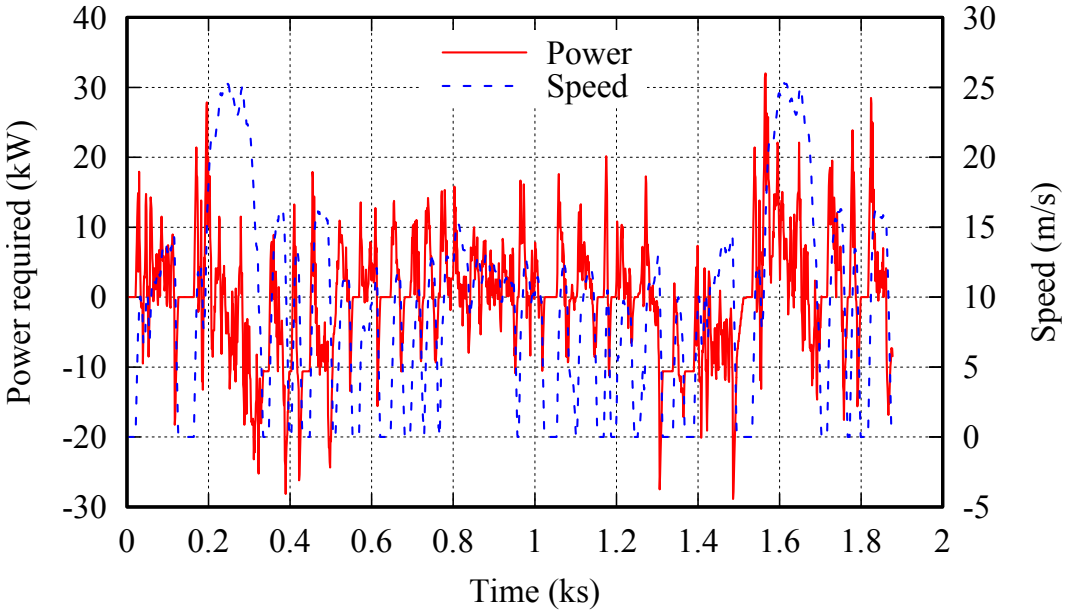

Figure 4.1. Power requirement and speed relationship for FTP-75.

The highway drive cycle shown in Figure 4.2 provides some interesting information. From about 600 s to 720 s in the plot, it is observed that the power requirement has increased, but the speed the vehicle is travelling at is still relatively constant. This could indicate a typographical change such as an inclination of the road. This would require more power from the vehicle to maintain its current speed.

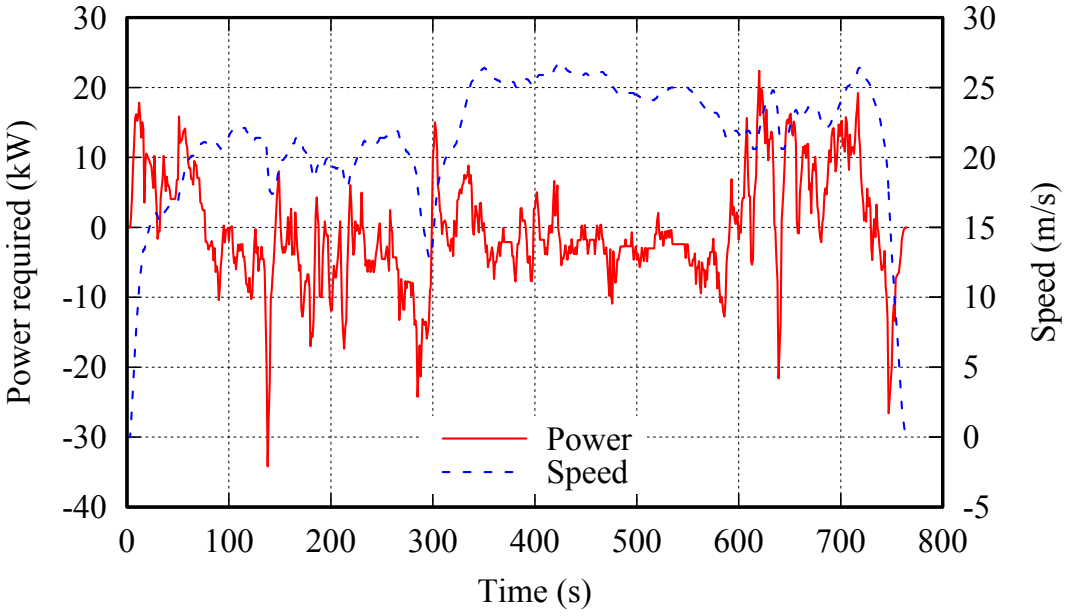

Figure 4.2. Power requirement and speed relationship for FTP-Highway.

4.3 BATTERY USE

The following results show how the batteries were receiving and deploying power in each of the configurations.

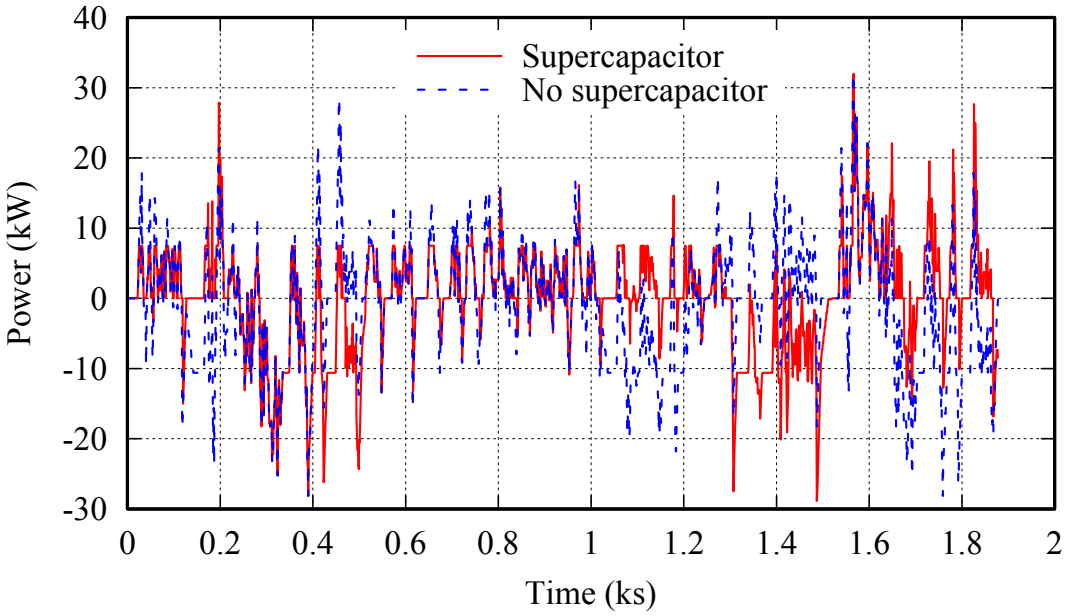

Figure 4.3. Battery use compared for FTP-75.

As it is slightly difficult to analyse the results in Figure 4.3, a zoomed-in version is produced in Figure 4.4. This gives a detailed presentation of how the batteries in both configurations were utilised. The focus is from 400 to 750 s of the drive cycle, entering the phase where it could be perceived that there were no differences between the graphs.

With the graph zoomed in it becomes evident that the supercapacitor and power distribution controller is acting as expected by limiting the battery power to 7.5 kW and the supercapacitor supplying the rest of the power required. This should be very beneficial for the battery in terms of life and thermal efficiency, since the current drawn can be significantly less than without the temporary energy storage.

In Figure 4.5 the power use graphs between the system with and without a supercapacitor are almost identical. This is due to the velocity of the vehicle not fluctuating nearly as much as in an urban environment. Thus resulting in the battery being the main power source throughout the highway cycle.

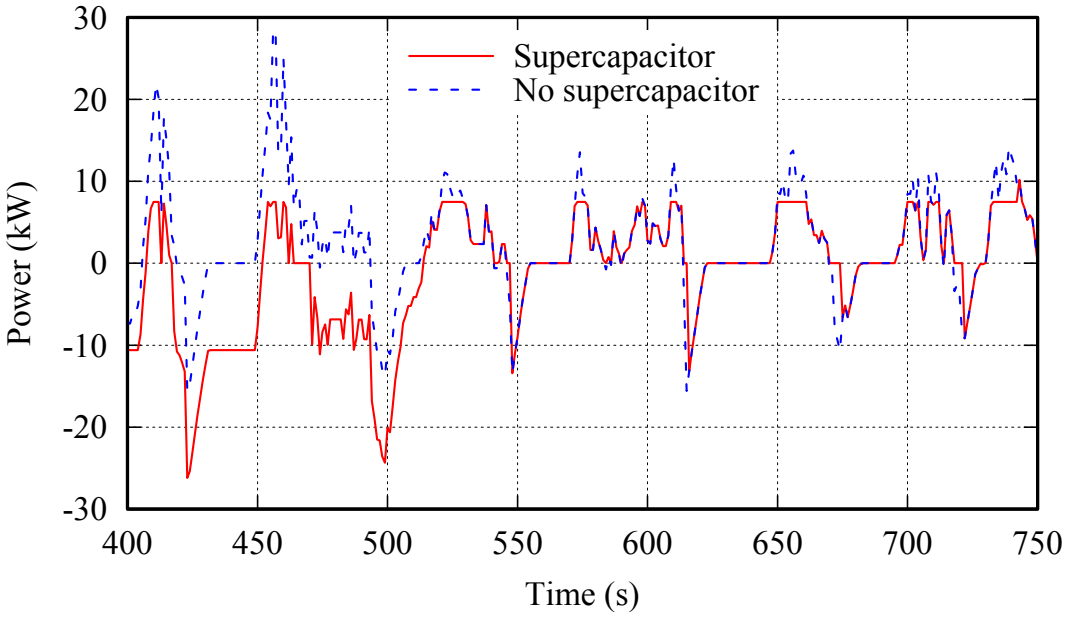

Figure 4.4. Zoomed in version of Figure 4.3 from 400 s to 750 s.

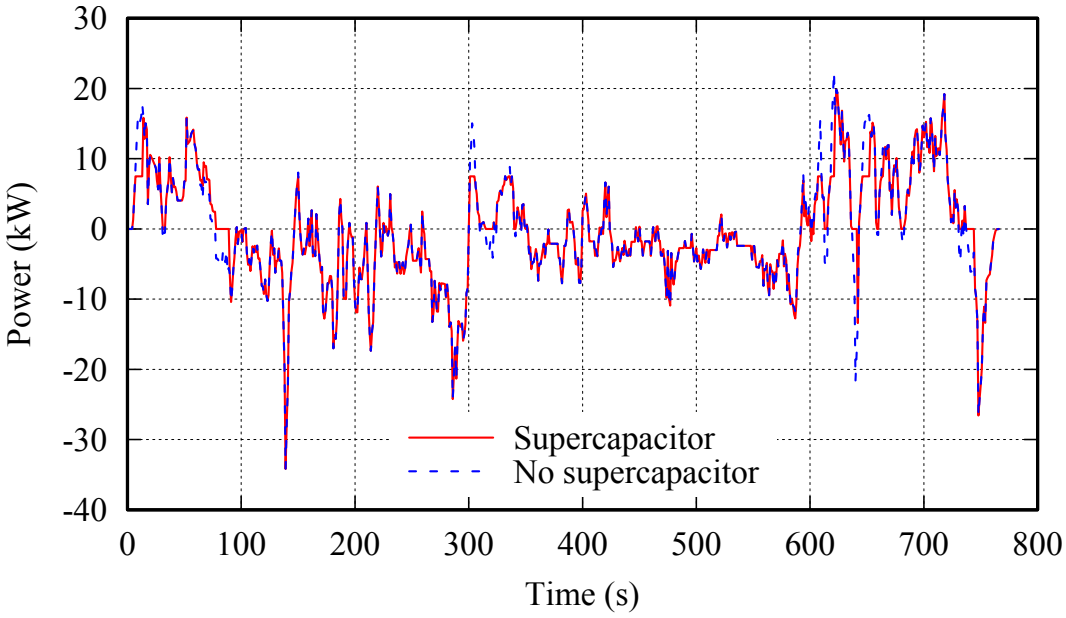

Figure 4.5. Battery use compared for FTP-Highway.

Based on the results in Figure 4.3 and 4.5, it was determined that the supercapacitor has limited the battery power output to the preset cut-off amount for 183 s of the FTP-75 drive cycle, and 32 s during the highway drive cycle. This means that the supercapacitor is a lot more effective in assisting the battery in an urban environment compared to highway driving.

4.4 POWER DISTRIBUTION BETWEEN BATTERY AND SUPERCAPACITOR

These results illustrate the power distribution performed by the controller to maximise the use of the supercapacitor for any power requirements above 7.5 kW whilst ensuring the supercapacitor is not used unless it has sufficient charge. The total power requirement is included as the combined power to prove that the sum of the battery and supercapacitor power flow meets these requirements.

It can be observed from Figure 4.6 that the supercapacitor is used very actively during an urban drive. It can be seen that frequently the battery did not have to deliver power exceeding 7.5 kW, only in very demanding instances.

As expected, Figure 4.7 shows that the highway drive cycle is significantly less demanding in terms of stopping and accelerating and therefore the supercapacitor is rarely utilised.

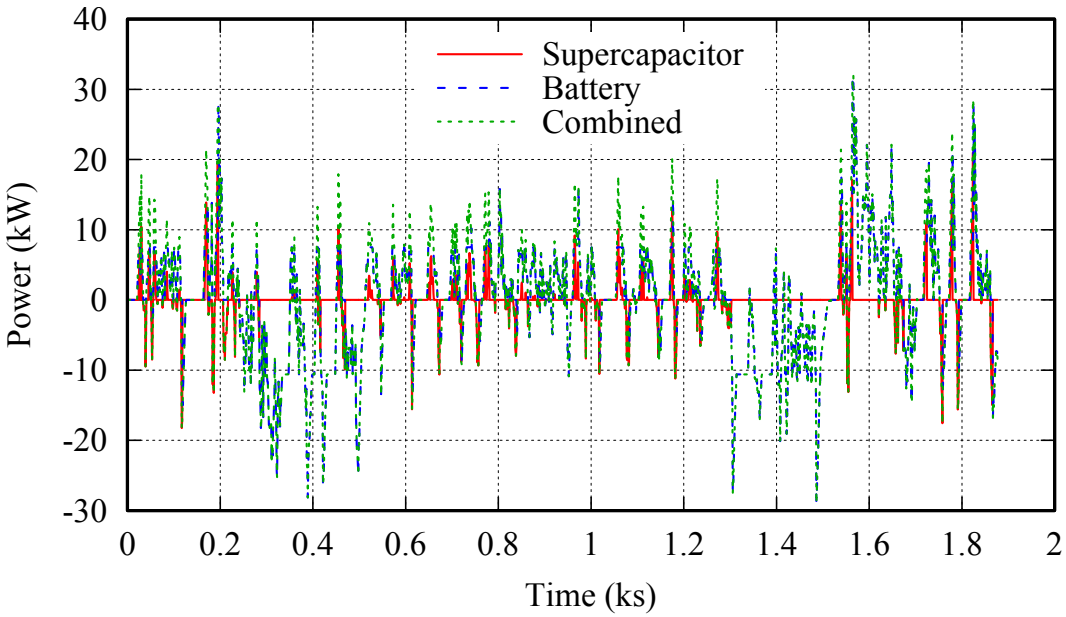

Figure 4.6. Power distribution performed by controller for FTP-75.

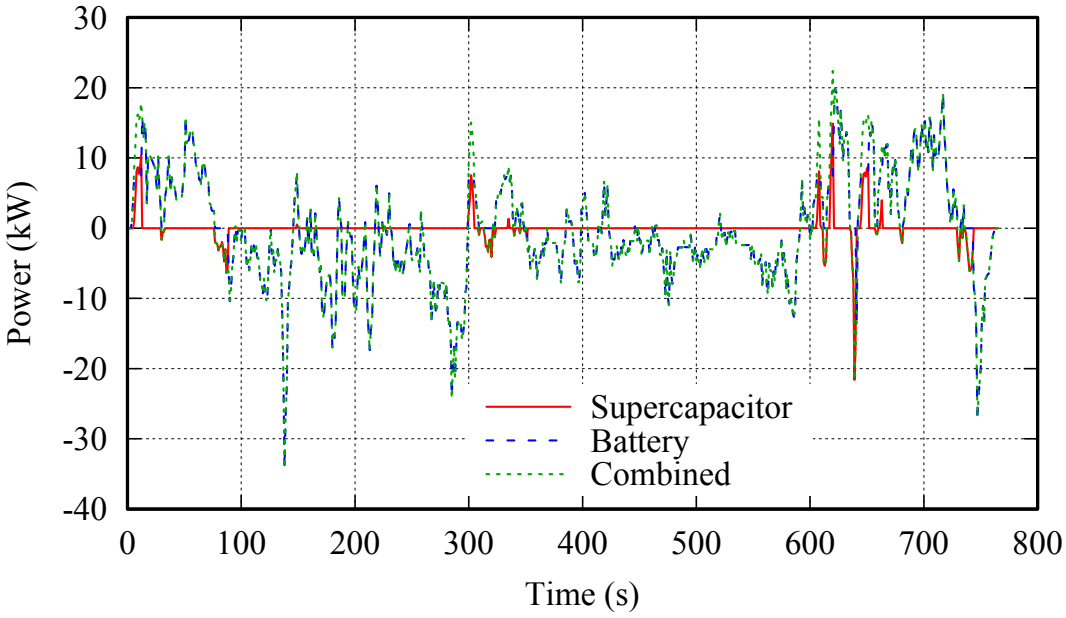

Figure 4.7. Power distribution performed by controller for FTP-Highway.

4.5 ENGINE UTILISATION

This section of the results shows when the battery charge was depleted and the ICE was needed as a range extender to charge the battery. This would indicate if there is a reduction in fuel consumption and emissions between the two configurations.

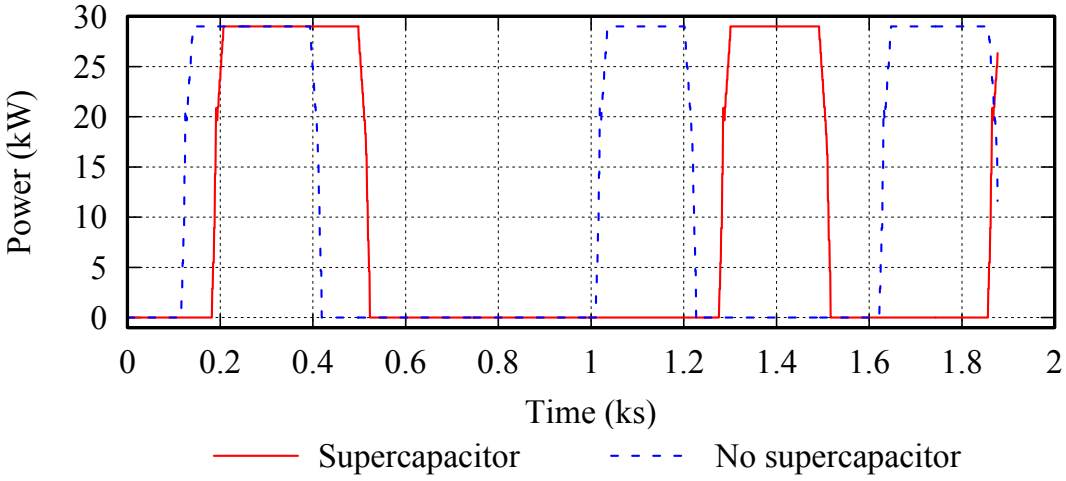

Figure 4.8. Engine utilisation comparison for FTP-75.

The results for the FTP-75 drive cycle show a significant difference between the different models. The

vehicle without the supercapacitor had to utilise the ICE three times during the FTP-75 drive cycle, and the engine was still in the ramp-down phase to shut off. The vehicle with the supercapacitor only used the ICE twice and just started the engine at the end of the cycle. This will decrease emissions of the vehicle in an urban driving environment.

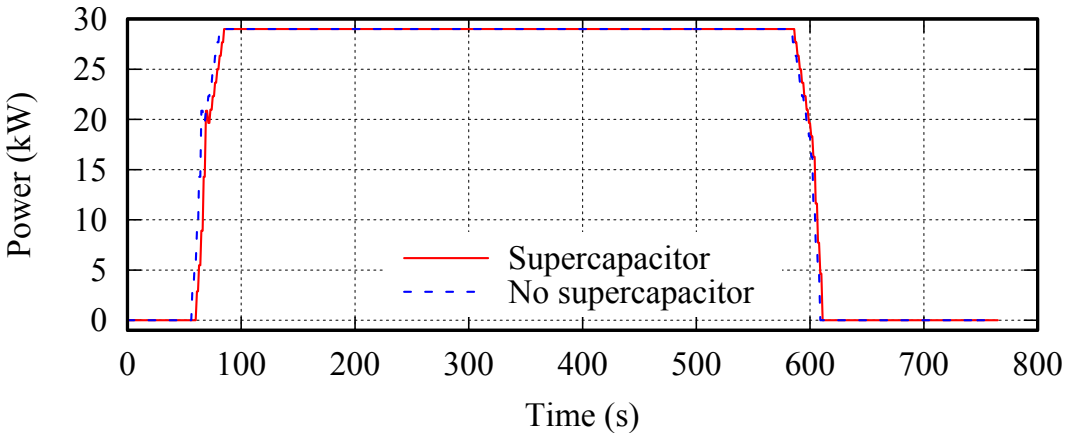

Figure 4.9. Engine utilisation comparison for FTP-Highway.

There are not any notable changes during the highway drive cycle due to the supercapacitor not being as effective in more constant velocity scenarios. It is visible that the vehicle with the supercapacitor utilised the ICE for a marginally shorter time.

4.6 BATTERY STATE OF CHARGE

Analysing the state of charge graphs will provide insight into how much the battery was discharged and will show the impact the additional energy-storage system had.

From Figure 4.10 we can immediately conclude that the battery discharge rate was significantly less with the presence of a supercapacitor. From 500 s to 1 300 s of the cycle where lots of acceleration and deceleration took place, the supercapacitor reduced the battery's discharge rate. This is linked to the instances where the peak shaving took place as seen in Figure 4.4. This delayed discharge the point of minimum SOC at which the battery needed to be recharged by almost 300 s. The battery in the system without the supercapacitor completed three full charge cycles, whereas the system with the supercapacitor managed to complete the drive cycle with only two full charges. That is a clear improvement in terms of the battery life expectancy since Li-ion batteries degrade to a point where they are no longer efficient. This is known as the cycle count which could be up to 10 000 for Li-ion

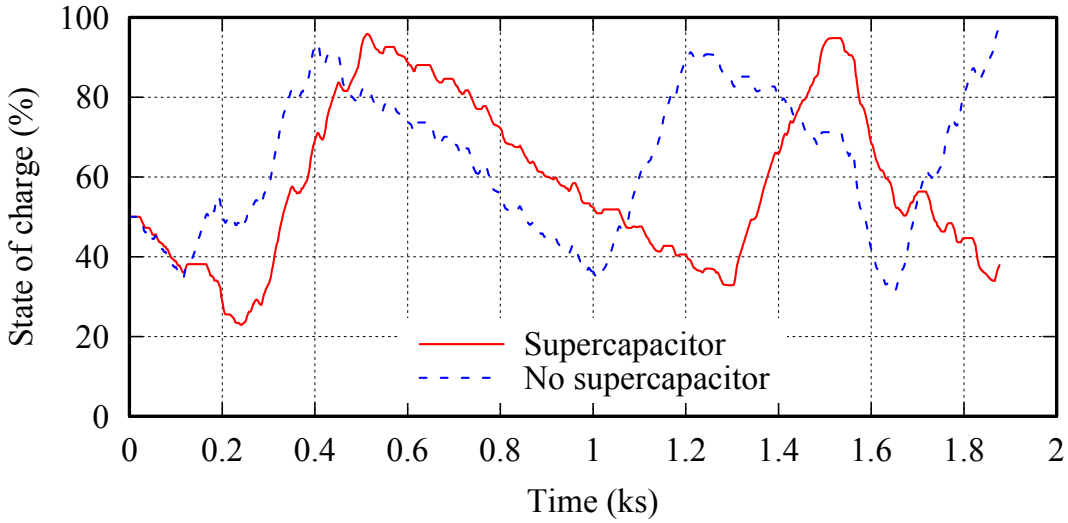

Figure 4.10. The state of charge of the battery for FTP-75.

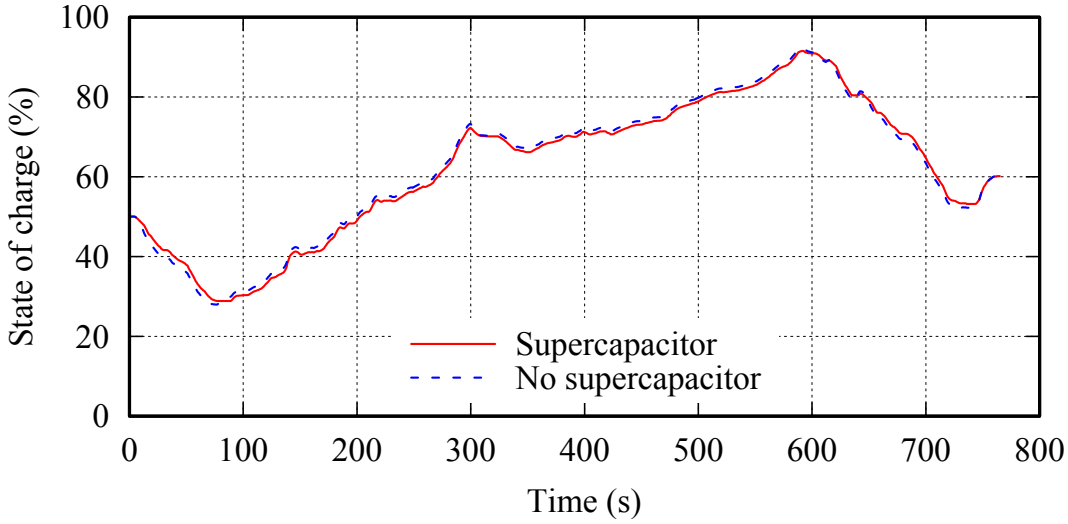

Figure 4.11. The state of charge of the battery for FTP-Highway.

batteries, which is much less in comparison to about 500 000 cycles capability of supercapacitors. By reducing the number of cycles required, the battery life can be extended.

Once again there was no major difference in the highway setting, with the SOC of both configurations nearly identical throughout the drive cycle.

4.7 FUEL ECONOMY AND EMISSIONS

The results of the reference model without a supercapacitor and the proposed model with the addition of the supercapacitor are summarised in Table 4.1. The combined fuel consumption is simply the average value between the two drive cycles. This terminology is commonly used in the automotive industry, to convey the expected fuel consumption when the vehicle is used for both city and highway driving. It also reveals that the reference vehicle was able to achieve almost identical fuel consumption to what was specified in Section 3.2.6.

Table 4.1. Fuel economy comparison.

Parameter	Supercapacitor	
	Without	With
FTP-75 (L/100 km)	3.71	2.85
FTP-Highway (L/100 km)	2.95	2.94
Combined (L/100 km)	3.33	2.90

Table 4.2 provides a summary of the fuel used and emissions emitted by the HEV in both drive cycles. First without the supercapacitor, and then with the supercapacitor added to the model. The simulation model calculates the fuel consumption (L/100 km) displayed in Table 4.1, since the distance (km) of the correlating drive cycle is known, the fuel consumed (L) is determined by (4.1). The emitted mass for each individual emission is calculated by (4.2), where the fuel consumed is multiplied with each of the emission baselines of Table 3.4.

Table 4.2. Emissions results for each drive cycle and configuration.

	Fuel Consumed (L)	CO2 (kg)	CO (g)	THC (mg)	NOx (mg)
FTP-75 Without Supercapacitor	0.660	2.24	2.97	492.0	190.0
FTP-Highway Without Supercapacitor	0.525	1.78	2.37	391.4	151.1
FTP-75 With Supercapacitor	0.507	1.72	2.28	378.0	146.0
FTP-Highway With Supercapacitor	0.485	1.65	2.19	361.6	139.6

$$\text{Fuel consumed (L)} = \frac{\text{Fuel economy (L/100 km)}}{100} \times \text{Distance (km)} \tag{4.1}$$

$$\text{Emitted mass} = \text{Fuel consumed (L)} \times \text{Corresponding baseline of Table 3.4} \tag{4.2}$$

The results summarised in Table 4.1 and 4.2 show that fuel consumption could be improved by up to 23%, which also ensured that emissions could be reduced with a similar percentage. The noted decrease in emissions can be observed especially during the urban drive cycle. The additional storage system is evidently successful in reducing fuel consumption and emissions.

4.8 SUMMARY

Most of the results are presented in such a way that the comparison is easy to see between the reference and proposed models. It is evident that the proposed vehicle outperforms the reference vehicle in every plot or table summarised with results. This is especially the case when the urban driving cycle was used. This means that the benefit of an additional supercapacitor is most evident in a city driving environment. The proposed model proved that it could reduce the strain on the battery during high power demand. This results in a smoother decrease in battery charge and an increase in travelling range and battery longevity. The engine was utilised for less time during a drive cycle, using less fuel and producing fewer emissions. The overall improvement achieved based on results is about 23%.

CHAPTER 5 DISCUSSION

5.1 CHAPTER OVERVIEW

The cost and environmental benefits of adding a supercapacitor to a HEV will be discussed in this section. The benefits are outlined based on the fuel cost, emissions and battery service life.

5.2 FUEL COST BENEFIT

The HEV with the additional short-term energy storage solution is definitely showing improved results, especially in an urban driving environment where frequent acceleration and deceleration take place. Thus proving that the power peak shaving approach to implementing the supercapacitor was successful.

It is stated in the specification that the Toyota Yaris Hybrid contains a 36 L fuel tank [37]. The original combined fuel consumption was 3.3 L/100 km, ensuring a theoretical range of 1 090.90 km from a full tank. The vehicle with the supercapacitor obtained a fuel consumption of 2.9 L/100 km, increasing the theoretical range to 1 241.38 km from a full tank.

If a person would travel an average of about 20 000 km per year, after 5 years using the combined fuel economy, the fuel used would be 3 300 L and 2 900 L without and with a supercapacitor, respectively. The use of a supercapacitor thus reduces fuel consumption by 400 L over a 5-year period, and with the price of fuel in South Africa being 26.31 South African Rand (ZAR)/L at the time of compiling this article in July 2022, this provides a potential fuel cost saving of 10 524.00 ZAR

5.3 IMPACT ON EMISSIONS

Modern vehicles bought are all subjected to emissions tax. This tax is determined by the CO_2 emissions emitted per kilometre by the ICE. In this study, the CO_2 emission has reduced from 112 g/km for the reference model to 98.6 g/km for the proposed model.

The emissions fee based on the South African Revenue Service (SARS) vehicle emissions tax outline is 132.00 ZAR for any passenger vehicle with a CO_2 classification above 95 g/km [41]. The reference vehicle would be taxed 14 784 ZAR and the proposed vehicle 13 015.20 ZAR, this is a saving of 1 768.80 ZAR.

Through further optimisation of this concept, the CO_2 emissions could actually be reduced to under the 95 g/km threshold where there would be no tax applied. Saving up to 14 784.00 ZAR.

5.4 BATTERY LONGEVITY

The battery completes 4 full charges when travelling 34.26 km (sum of the urban and highway drive cycles) with the vehicle without a supercapacitor. Based on knowledge from Section 2.3.1 the battery can last about 10 000 cycles, meaning the battery would last for 85 650 km. The vehicle with the supercapacitor completes 3 full charges when travelling that same distance, therefore would have completed 114 200 km before reaching its end of life. Assuming the vehicle travels an annual distance of 20 000 km, the battery in the vehicle without a supercapacitor will last just over 4 years. The battery in the vehicle with the supercapacitor has extended that to almost 6 years before requiring a replacement.

5.5 COMPARISON TO SIMILAR STUDIES

Finding studies with enough similarities to compare with this study proved to be rather difficult. In most cases, there were no numerical results published, however, some of the studies mentioned observations such as the supercapacitor is capable of supporting the battery to reduce peak current. The studies reported increased battery life, decreased fuel consumption and emissions and increased travelling range [42–44]. Which is equal to the observations documented in this dissertation.

As introduced in Section 2.4 study [29] used the QSS approach, but used outdated components and neglected control strategies. The results however showed that improvements in fuel consumption is definitely possible with a reported decrease between 30.2% and 31.3%. The study unfortunately did not consider the battery life or emissions, so cannot be compared.

A study conducted on microcars, where a HESS with a Li-ion battery and supercapacitor was implimented, showed similar results. The study reported that the supercapacitor had similarly aided the battery during high power demand instances, which reduced the degradation of the battery and decreased battery operating temperature. The results proved that fuel consumption was decreased by up to 28% for city driving and the battery service life increased by more than 40%. Numerical results for emissions were unfortunately not provided [45].

5.6 SUMMARY

This chapter shows that the results obtained are positive. The results were discussed from the viewpoint of what the improvements have to offer over the reference vehicle. The discussion shows clear increases in battery service life and vehicle range before battery health could be declining to a point of concern. The costs of adding a supercapacitor to the system are largely covered by the savings on fuel and the potential to avoid going above the tax emissions threshold with some optimisation. A summary of other similar studies were presented and by comparison showed that the results obtained in this study are sensible.

CHAPTER 6 CONCLUSION

6.1 CONCLUDING REMARKS

The experiment was very successful. It was possible to use the QSS toolbox simulation software to perform all the necessary steps to achieve the goals of this study. The software is extremely flexible and easy to use once figured out. The models were updated to modern technology to ensure the results are comparable to current real-world HEVs. This included remodelling the lead acid battery to Li-ion, and the battery controller to perform dynamic operations instead of preset time-based charging. A new series HEV configuration was introduced with an additional supercapacitor added to work in parallel with the battery. This required the modelling of a power management controller to use a peak power shaving method to eliminate high power draws from the battery.

The results show that this approach was successfully executed. The battery remained at the preset cutoff power while the supercapacitor supplied the remaining power required. This also improved fuel consumption by about 23% and reduced emissions by that same amount. As expected the effect of the additional storage system was much more noticeable during city driving. The travelling range on a full tank of fuel has also increased by almost 13%. Lower battery use had a very positive effect on the service life of the battery, adding 28 550 km to its total range. This means battery longevity increased by 33%.

The results obtained show that the addition of a temporary energy storage system is a good concept. Even with the supercapacitor only having about 5% of the energy storing capacity of the Li-ion battery. The cost of implementing this concept could arguably be justified by all the advantages and benefits it has. Although the supercapacitor unit is priced at 2 563.17 USD (41 010.72 ZAR at 16 ZAR/USD) to the general public, when the vehicle manufacturer decides to use such a concept, they would surely be capable of implementing it in a much more cost-effective manner. It was also discussed that cost

savings on the vehicle's emissions tax are present, and could potentially eliminate the tax through further optimisation of the model.

6.2 FUTURE STUDIES

This study covered quite a substantial number of different aspects of HEVs. There are still a lot of other elements that could be investigated. A further study could include an optimisation model to determine the best cost-to-benefit ratio to assist in sizing the supercapacitor.

A completely different approach could be taken that might consider the thermal implications of this configuration. Or even a deeper dive into the HESS alone, to determine a layered configuration, where rows or columns of Li-ion cells could be split by supercapacitor cells to create a single package.

The same study could be implemented with a different HEV configuration such as a parallel HEV model and also a series-parallel combination.

A different power management control technique could be implemented, these include fuzzy logic control, neural network or model predictive control [28]. A study could be implemented to perform a prediction of the route, to determine the optimal strategy of energy use between the two energy storage systems. It is however unclear how well this would work in a QSS environment since it is already a backwards simulation method, where some of the input variables must be provided before the simulation can begin. This could still be done in a different simulation package where a dynamic method is used. From a practical perspective, this study is valid, since the prediction could resemble the route programmed into the Global Positioning System (GPS) navigation system of the vehicle.

REFERENCES

[1] A. A. Adeyanju and K. Manohar, "Effects of Vehicular Emission on Environmental Pollution in Lagos," *Sci-Afric Journal of Scientific Issues, Research and Essays*, vol. 5, no. 4, pp. 34–51, Apr. 2017.

[2] P. G. Kumar, P. Lekhana, M. Tejaswi, and S. Chandrakala, "Effects of vehicular emissions on the urban environment- a state of the art," *Materials Today: Proceedings*, vol. 45, pp. 6314–6320, Dec. 2020.

[3] M. O. Dioha, J. Lukuyu, E. Virgüez, and K. Caldeira, "Guiding the deployment of electric vehicles in the developing world," *Environmental Research Letters*, vol. 17, no. 7 (071001), pp. 1–5, Jun. 2022.

[4] L. Bokopane, K. Kanzumba, and H. Vermaak, "Is the South African Electrical Infrastructure Ready for Electric Vehicles?" in *2019 Open Innovations Conference, OI 2019*, Cape Town, South Africa, Oct. 02-04 2019, pp. 127–131.

[5] M. I. Tongwane and M. E. Moeletsi, "Status of electric vehicles in South Africa and their carbon mitigation potential," *Scientific African*, vol. 14, no. e00999, pp. 1–12, Nov. 2021.

[6] G. Pignatta and N. Balazadeh, "Hybrid Vehicles as a Transition for Full E-Mobility Achievement in Positive Energy Districts: A Comparative Assessment of Real-Driving Emissions," *Energies*, vol. 15, no. 2760, pp. 1–18, Apr. 2022.

[7] L. Tang, G. Rizzoni, and S. Onori, "Energy management strategy for HEVs including battery life optimization," *IEEE Transactions on Transportation Electrification*, vol. 1, no. 3, pp. 211–222, Oct.

[8] G. Rizzoni, L. Guzzella, and B. M. Baumann, "Unified modeling of hybrid electric vehicle drivetrains," *IEEE/ASME Transactions on Mechatronics*, vol. 4, no. 3, pp. 246–257, Sep. 1999.

[9] F. Mangun, M. Idres, and K. Abdullah, "Design optimization of a hybrid electric vehicle powertrain," in *IOP Conference Series: Materials Science and Engineering*, vol. 184, no. 012024, Kuala Lumpur, Malaysia, Jul. 25-27 2016, pp. 1–7.

[10] W. Weerasinghe, R. Stobart, and S. Hounsham, "Thermal efficiency improvement in high output diesel engines a comparison of a rankine cycle with turbo-compounding," *Applied Thermal Engineering*, vol. 30, no. 14, pp. 2253–2256, Oct. 2010.

[11] F. Irani, "On dynamic programming technique applied to a parallel hybrid electric vehicle," Master's thesis, Chalmers University of Technology, 2009.

[12] M. Ramesh, "Optimization of hybrid driveline configuration," Master's thesis, Chalmers University of Technology, 2018.

[13] L. Sun, N. Zhang, M. Awadallah, and P. Walker, "An innovative control strategy for a hybrid energy storage system (hess)," in *2017 IEEE International Conference on Mechatronics (ICM)*, Churchill, VIC, Australia, Feb. 13-15 2017, pp. 434–439.

[14] Z. Cabrane, J. Kim, K. Yoo, and M. Ouassaid, "Hess-based photovoltaic/batteries/supercapacitors: Energy management strategy and dc bus voltage stabilization," *Solar Energy*, vol. 216, pp. 551–563, Mar. 2021.

[15] L. Guzzella and A. Sciarretta, *Vehicle propulsion systems: Introduction to modeling and optimization*. Berlin Heidelberg, Germany: Springer, 2005.

[16] K. S. Boparai and R. Singh, "Electrochemical energy storage using batteries, superconductors and hybrid technologies," in *Encyclopedia of Renewable and Sustainable Materials*. Oxford, United Kingdom: Elsevier, 2020, vol. 1, pp. 248–254.

[17] S. Muench, A. Wild, C. Friebe, B. Häupler, T. Janoschka, and U. S. Schubert, "Polymer-based organic batteries," *Chemical Reviews*, vol. 116, no. 16, pp. 9438–9484, Aug. 2016.

[18] K. Itani, A. De Bernardinis, Z. Khatir, and A. Jammal, "Comparative analysis of two hybrid energy storage systems used in a two front wheel driven electric vehicle during extreme start-up and regenerative braking operations," *Energy Conversion and Management*, vol. 144, pp. 69–87, Jul. 2017.

[19] M. G. Molina, "Energy Storage and Power Electronics Technologies: A Strong Combination to Empower the Transformation to the Smart Grid," *Proceedings of the IEEE*, vol. 105, no. 11, pp. 2191–2219, Nov. 2017.

[20] "Lamborghini SIAN FKP 37," Lamborghini, Nov. 14 2021. [Online]. Available: https://www.lamborghini.com/en-en/models/limited-series/sian-fkp-37

[21] F. Barzegar, "Supercapacitors or batteries," SA Energy Storage Conference Presentation, Ekurhuleni, South Africa, Sep. 22-23 2018. [Online]. Available: https://www.ee.co.za/wp-content/uploads/2018/10/Dr-Farshad-Barzegar-University-of-Pretoria-presentation.pdf

[22] M. Pershaanaa, S. Bashir, S. Ramesh, and K. Ramesh, "Every bite of supercap: A brief review on construction and enhancement of supercapacitor," *Journal of Energy Storage*, vol. 50, p. 104599, Jun. 2022.

[23] "Eaton XVM-259 supercapacitor," data sheet, Eaton, Cleveland, OH, USA, Jun. 2019, pub. no. 10920 BU-MC19055. [Online]. Available: https://www.eaton.com/content/dam/eaton/products/electronic-components/resources/data-sheet/eaton-xvm-259-pcba-supercapacitor-module-data-sheet.pdf

[24] N. Benyahia, H. Denoun, M. Zaouia, S. Tamalouzt, M. Bouheraoua, N. Benamrouche, T. Rekioua, and S. Haddad, "Characterization and control of supercapacitors bank for stand-alone photovoltaic energy," *Energy Procedia*, vol. 42, pp. 539–548, Nov. 2013.

[25] M. A. Conteh and E. C. Nsofor, "Composite flywheel material design for high-speed energy storage," *Journal of Applied Research and Technology*, vol. 14, no. 3, pp. 184–190, Jun. 2016.

[26] N. Hashemnia and B. Asaei, "Comparative study of using different electric motors in the electric vehicles," in *Proceedings of the 2008 International Conference on Electrical Machines, ICEM'08*, no. c, Vilamoura, Portugal, Sep. 06-09 2008, pp. 1–5.

[27] J. Ko, S. Ko, H. Son, B. Yoo, J. Cheon, and H. Kim, "Development of brake system and regenerative braking cooperative control algorithm for automatic-transmission-based hybrid electric vehicles," *IEEE Transactions on Vehicular Technology*, vol. 64, no. 2, pp. 431–440, Feb. 2015.

[28] U. Manandhar, A. Ukil, S. K. Kollimalla, and H. B. Gooi, "Application of hess for pv system with modified control strategy," in *2015 IEEE Innovative Smart Grid Technologies - Asia (ISGT ASIA)*, Bangkok, Thailand, Nov. 03-06 2015, pp. 1–5.

[29] W. F. Infante, A. F. Khan, N. J. C. Libatique, G. L. Tangonan, and S. N. Y. Uy, "Performance evaluation of series hybrid and pure electric vehicles using lead-acid batteries and supercapacitors," in *IEEE Region 10 Annual International Conference, Proceedings/TENCON*, Cebu, Philippines, Nov. 19-22 2012, pp. 1–5.

[30] A. Ostadi, M. Kazerani, and S. K. Chen, "Hybrid Energy Storage System (HESS) in vehicular applications: A review on interfacing battery and ultra-capacitor units," in *2013 IEEE Transportation Electrification Conference and Expo: Components, Systems, and Power Electronics - From Technology to Business and Public Policy, ITEC 2013*, Detroit, MI, USA, Jun. 16-19 2013.

[31] J. Shen, S. Dusmez, and A. Khaligh, "Optimization of sizing and battery cycle life in battery/ultracapacitor hybrid energy storage systems for electric vehicle applications," *IEEE Transactions on Industrial Informatics*, vol. 10, no. 4, pp. 2112–2121, Nov. 2014.

[32] M. Passalacqua, D. Lanzarotto, M. Repetto, L. Vaccaro, A. Bonfiglio, and M. Marchesoni, "Fuel economy and ems for a series hybrid vehicle based on supercapacitor storage," *IEEE Transactions on Power Electronics*, vol. 34, no. 10, pp. 9966–9977, Oct. 2019.

[33] "QSS toolbox," Swiss Federal Institute of Technology, Zürich, 2005. [Online]. Available: https://ethz.ch/content/dam/ethz/special-interest/mavt/dynamic-systems-n-control/idsc-dam/Research_Onder/Downloads/qss.zip

[34] "Vehicle and fuel emissions testing – dynamometer drive schedules." [Online]. Available: https://www.epa.gov/vehicle-and-fuel-emissions-testing/dynamometer-drive-schedules

[35] "Rechargeable lithium-ion battery MP 176065 HD integration," data sheet, Saft, Feb. 2009, doc. no. 54064-2-0209. [Online]. Available: http://www.saftlithium.nl/datasheets/BIN_2013MP_176065_INTEGRATION_HD.pdf

[36] S. Wilkinson, "Best-selling cars 2022: the UK's top 10 most popular models," Auto Express, England and Wales. [Online]. Available: https://www.autoexpress.co.uk/news/94280/best-selling-cars-2021

[37] "Yaris specs DEC2020," Specifications datasheet, Toyota Australia, Nov. 2020. [Online]. Available: https://www.toyota.com.au/-/media/toyota/main-site/vehicle-hubs/yaris/files/yaris_specs_dec2020.pdf

[38] "The all-new Toyota Yaris," Toyota Europe, Brussels, Belgium, Jul. 27 2020. [Online]. Available: https://newsroom.toyota.eu/the-all-new-toyota-yaris/

[39] "All new Toyota Yaris features & specifications," Toyota UK, 14 Nov. 2021. [Online]. Available: https://www.toyota.co.uk/new-cars/yaris/features-and-specs

[40] "Avnet," 2022. [Online]. Available: https://www.avnet.com/shop/emea/products/eaton/xvm-259r2425-r-3074457345643190519/

[41] "Environmental levy on carbon dioxide (CO_2) emissions of motor vehicles," data sheet, SARS, Apr. 2022, doc. no. 54064-2-0209. [Online]. Available: https://www.sars.gov.za/wp-content/uploads/Legal/SCEA1964/LAPD-LPrim-Tariff-2012-11-Schedule-No-1-Part-3D.pdf

[42] G. Subramanian and J. Peter, "Integrated li-ion battery and super capacitor based hybrid energy storage system for electric vehicles," in *2020 IEEE International Conference on Electronics, Computing and Communication Technologies (CONECCT)*, July 2020, pp. 1–6.

[43] A. K. Podder, O. Chakraborty, S. Islam, N. Manoj Kumar, and H. H. Alhelou, "Control strategies of different hybrid energy storage systems for electric vehicles applications," *IEEE Access*, vol. 9, pp. 51 865–51 895, March 2021.

[44] P. A. Wozniak, "Hybrid electric vehicle battery-ultracapacitor energy management system design and optimization," *Elektronika ir Elektrotechnika*, vol. 28, no. 1, pp. 4–15, February 2022.

[45] F. Ortenzi, N. Andrenacci, M. Pasquali, and C. Villante, "On the hybridization of microcars with hybrid ultracapacitors and li-ion batteries storage systems," *Energies*, vol. 13, no. 12, June 2020.

ADDENDUM A QSS TOOLBOX PARAMETERS AND SIMULINK MODELS

A.1 MODEL PARAMETERS

The tables that follow in this section are summaries of the parameters used in all the simulations. These values are inserted into the GUI masks of each component on the modelling page.

Table A.1. Vehicle model parameters.

Parameter	Value
Total vehicle mass	1200 kg
Rotating mass	5%
Vehicle cross section	2 m^2
Wheel diameter	0.5 m
Drag coefficient	0.22
Rolling friction coefficient	0.008

Table A.2. Transmission (vehicle to electric motor) model parameters.

Parameter	Value
Gear ratio	3.5
Efficiency	0.98%
Idling losses	300 W
Minimum wheel speed beyond which losses are generated	1 rad/s

Table A.3. Electric motor model parameters.

Parameter	Value
Motor scaling factor	3.5
Efficiency	0.1%
Power required by auxiliaries	0 W

Table A.4. Transmission (combustion engine to electric generator) model parameters.

Parameter	Value
Gear ratio	0.75
Efficiency	0.98%
Idling losses	200 W
Minimum wheel speed beyond which losses are generated	1 rad/s

Table A.5. Electric generator model parameters.

Parameter	Value
Generator scaling factor	2

Table A.6. Combustion engine model parameters.

Parameter	Value
Engine type	Otto
Engine displacement	1.5 L
Engine scaling factor	1
Engine inertia	0.05 kg$\cdot$ m^2
Engine speed at idle	105 rad/s
Engine power at idle	0 W
Power required by auxiliaries	0 W
Engine torque at fuel cutoff	0 Nm
Power at fuel cutoff	0 W

Table A.7. Power management controller model parameters.

Parameter	Value
Power at which capacitor does power shaving	7.5 kW

Table A.8. Supercapacitor model parameters.

Parameter	Value
Capacity of each supercap	4.17 F
Internal resistance of each supercap	0.310 Ω
Maximum voltage of supercap	259.2 V
Maximum power of each supercap	28 kW
Initial charge of each supercap	95%
Number of supercaps in parallel connection	1

Table A.9. Battery model parameters.

Parameter	Value
Initial charge of battery	0.5
Cells in series	48
Battery capacity	4.3 Ah

A.2 SIMULINK MODELS

Complete models in Simulink using the QSS toolbox. Figure A.1 is a screenshot of the battery controller model, the same model is used to control the supercapacitor as well, but with different parameters. The model presented in Figure A.3 is the power management controller introduced to manage the flow of power between the two energy storage systems. The model in Figure A.4 contains all the redesigned components as well as the additional supercapacitor, supercapacitor controller and power management controller. The blocks that are not filled with colour are new or updated models that are not part of the original QSS toolbox.

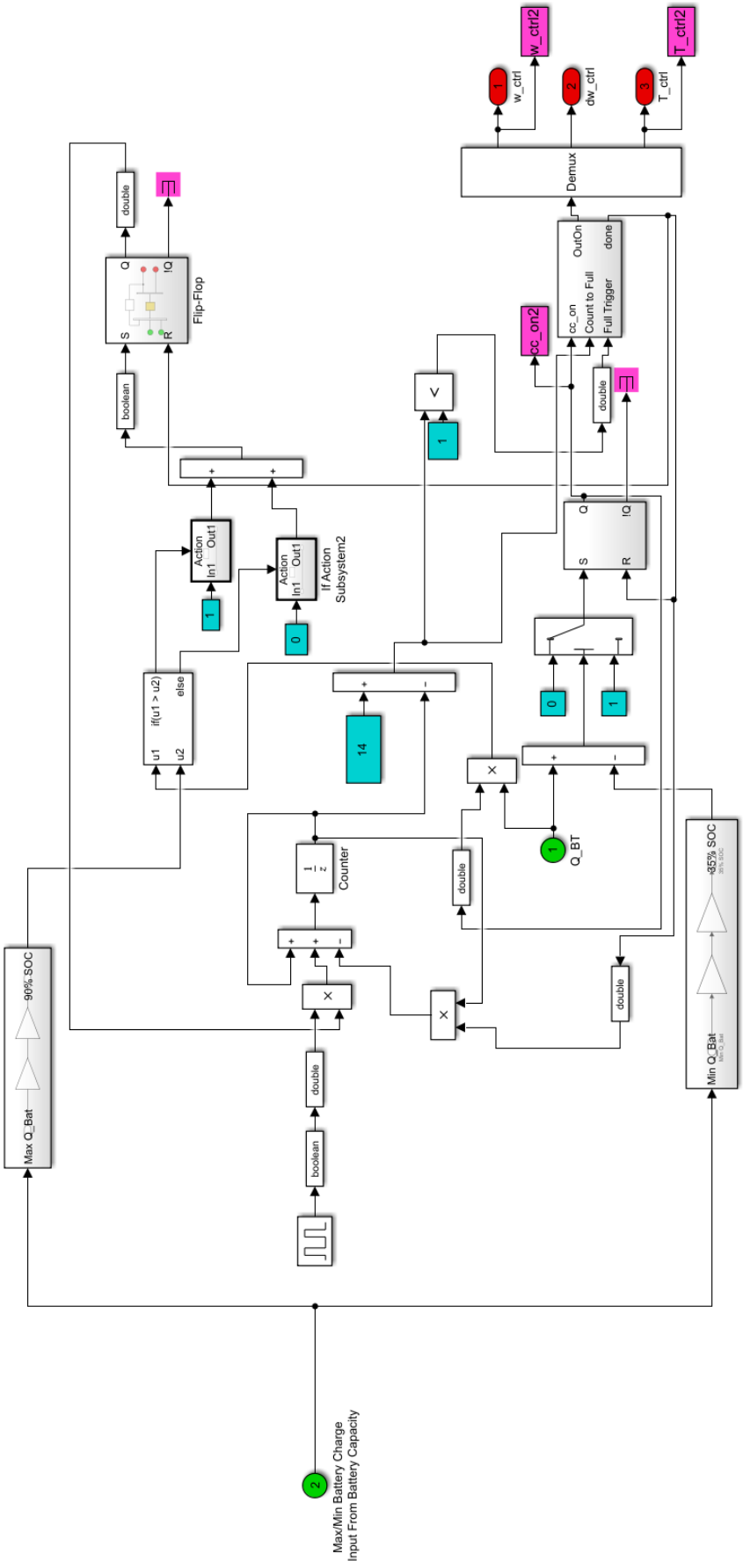

Figure A.1. A screenshot of the battery controller.

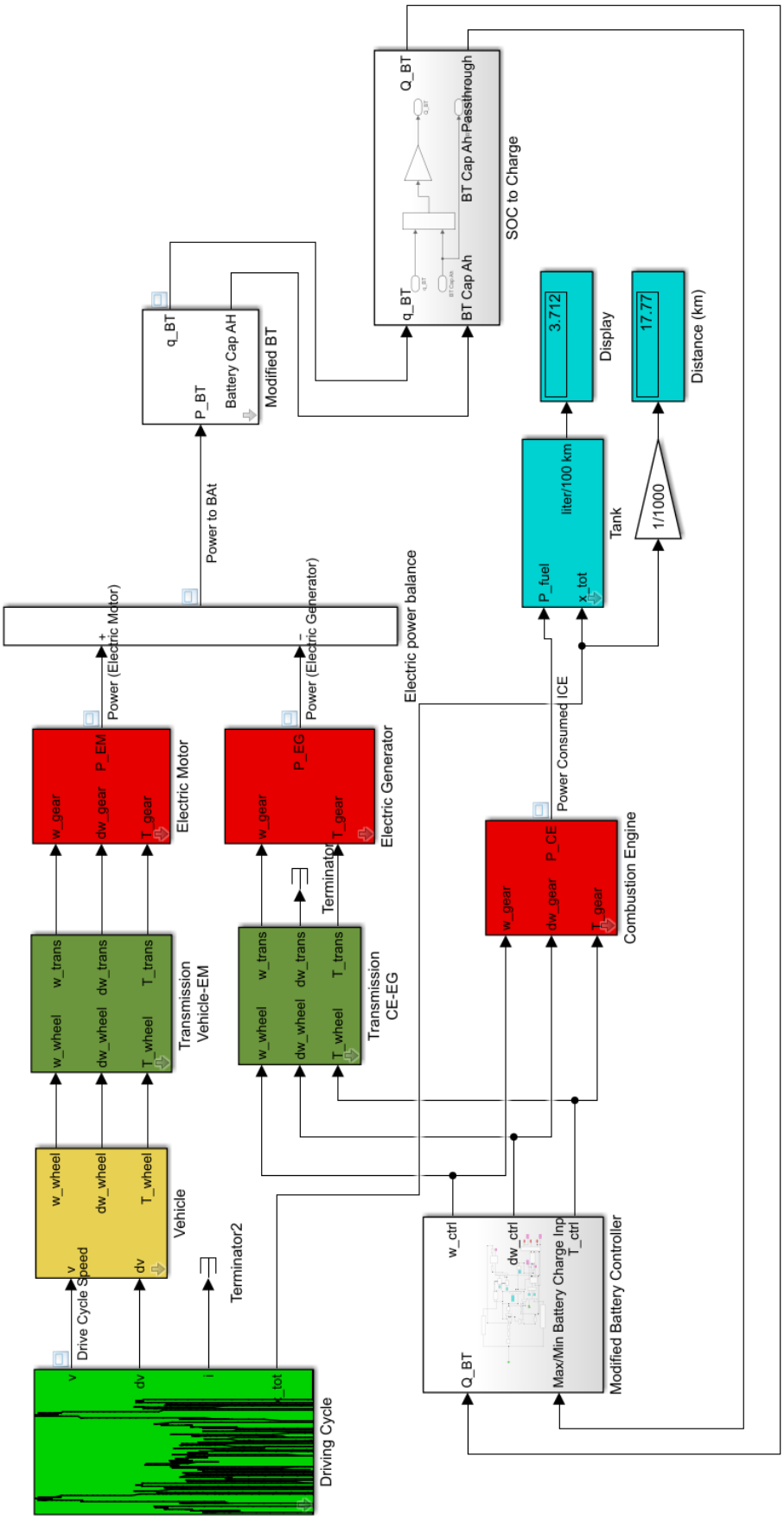

Figure A.2. A screenshot of the reference model.

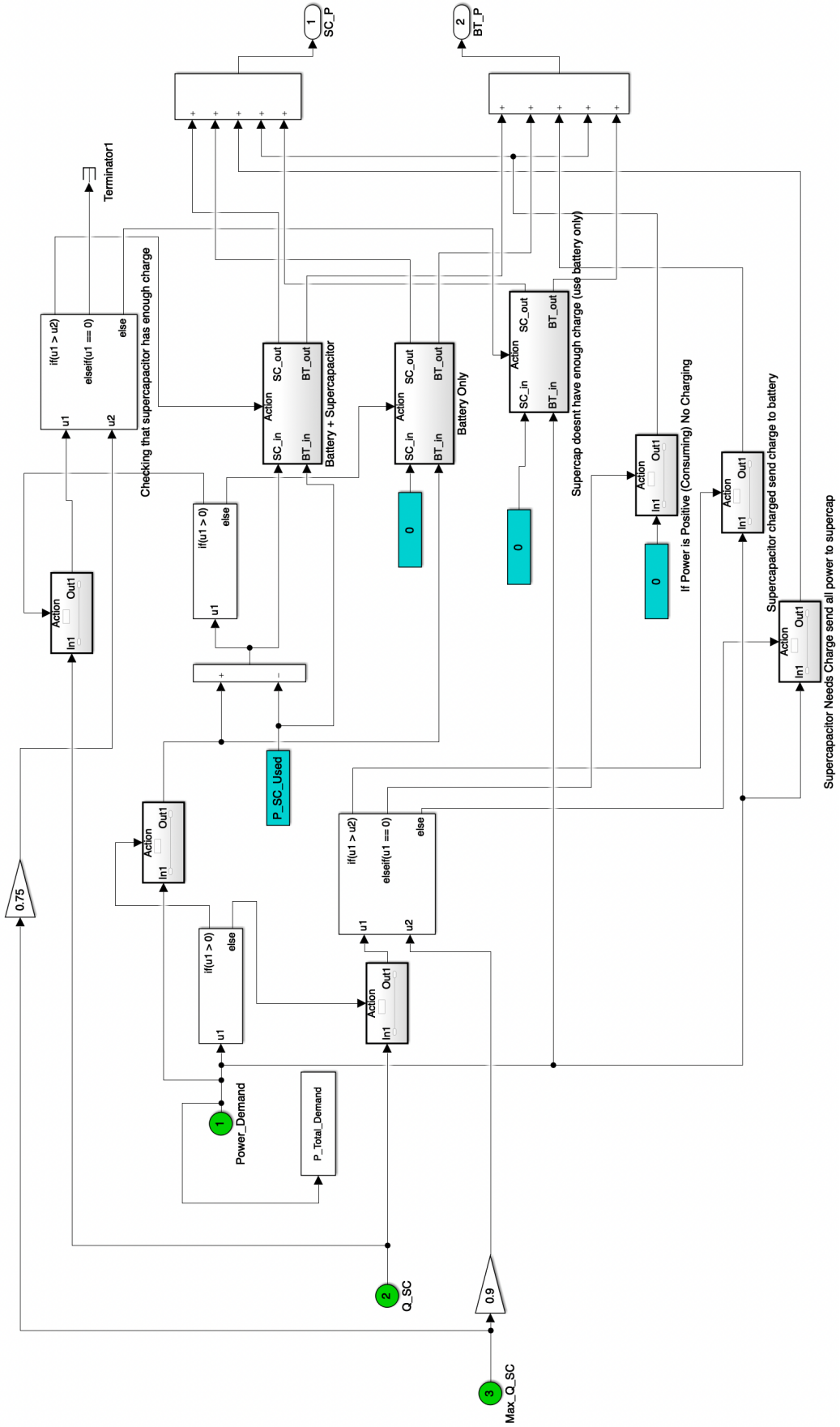

Figure A.3. A screenshot of the power management controller.

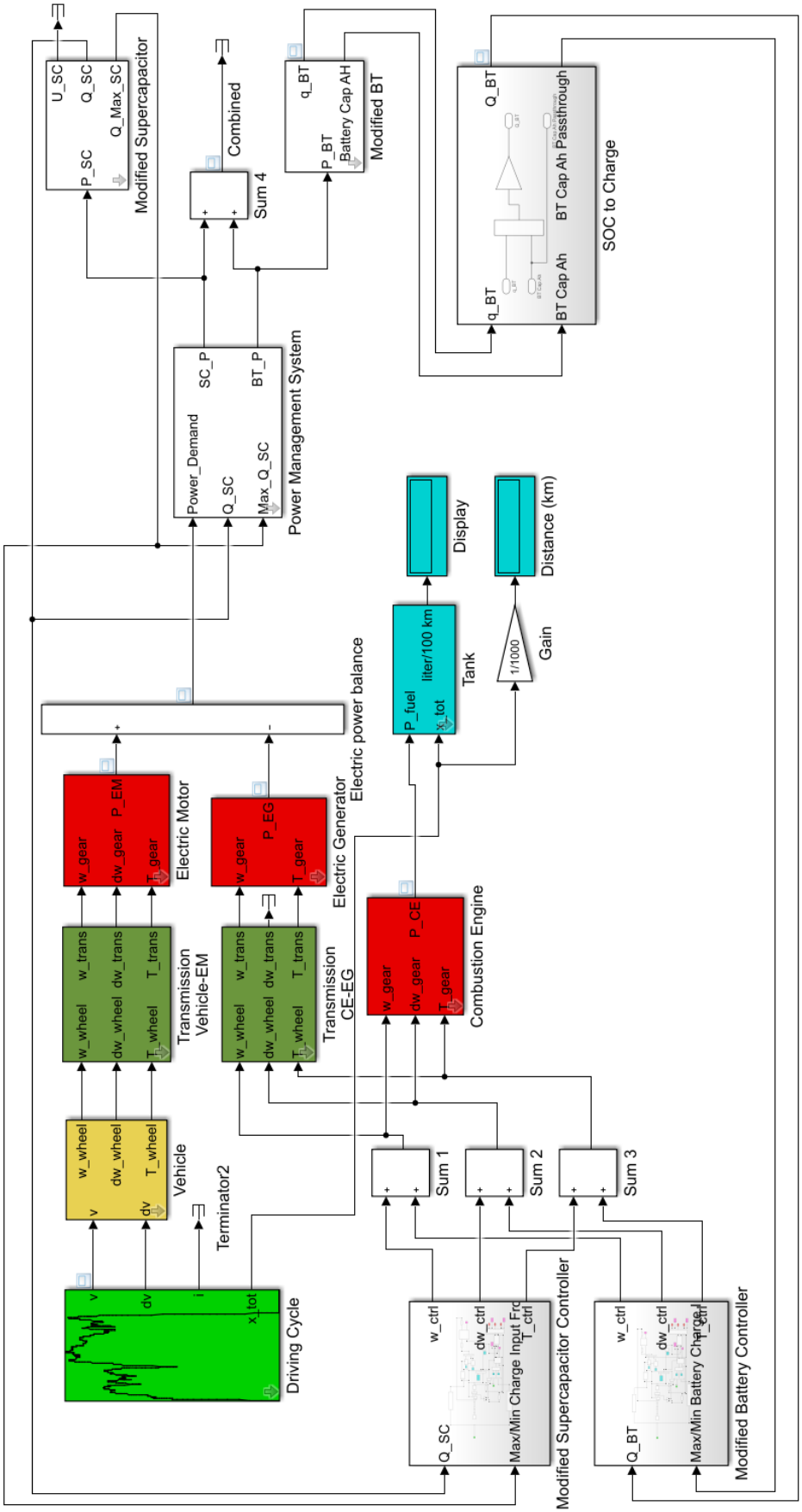

Figure A.4. A screenshot of the complete proposed series HEV model.